INVESTIGATION OF GREEN SYNTHESIZED SILVER NANOAPRTICLES USING AQUEOUS LEAF EXTRACT OF *ARTEMISIA ARGYI* FOR ANTIOXIDANT AND ANTIMICROBIAL POTENTIALS

By

HNG HUEY PING

A project report submitted to the Department of Chemical Science

Faculty of Science

Universiti Tunku Abdul Rahman

In partial fulfillment of the requirements for the degree of

Bachelor of Science (Hons) Biochemistry

May 2017

ABSTRACT

INVESTIGATION OF GREEN SYNTHESIZED SILVER NANOAPRTICLES USING AQUEOUS LEAF EXTRACT OF *ARTEMISIA ARGYI* FOR ANTIOXIDANT AND ANTIMICROBIAL POTENTIALS

HNG HUEY PING

The current study employs green synthesis to acquire silver nanoparticles (AgNPs) using *Artemisia argyi* and appraise their antioxidant and antimicrobial potentials. AgNPs were synthesized using aqueous leaf extract of *Artemisia argyi* by sunlight irradiation. They were characterized using UV-Vis spectrophotometer, FESEM, FTIR and XRD. The antioxidant capacity of AgNPs were evaluated using antioxidant assays including ABTS, DPPH, iron chelation, FRAP and NO radical scavenging methods. The antimicrobial activities were tested against *Esherichia coli* and *Staphylococcus aureus* using disc diffusion method. Descriptive statistical analysis was used to identify significant relationship between antioxidant activities of AgNPs. AgNPs exhibited brown color light scattering and absorbed maximum wavelength of light at 450 nm. The synthesis of AgNPs was optimum at 0.01 M $AgNO_3$. The green synthesized AgNPs were spherical in shape with size ranging from 16 nm to 32 nm. The FTIR analysis revealed the presence of proteins, phenolic and polar nitriles compounds in the AgNPs. The purified AgNPs possessed a

face centered cubic structure with coexistence of silver chloride crystals. The total phenolic and flavonoid of AgNPs was found to be 77.45 mg GAE/g AgNPs and 205.29 mg GAE/g AgNPs respectively. The radical scavenging activity (EC_{50}) showed highest activity for NO (31.33 µg/ml) followed by ABTS (128.82 µg/ml), DPPH (263.03 µg/ml) and Fe^{2+} (1445.44 µg/ml) with a FRAP value of 1.22 mmol Fe^{2+} /mg dry weight. AgNPs possessed inhibitory effect against both strains of bacteria in concentration dependent manner. Green synthesized AgNPs using *Artemisia argyi* are promising sources of effective antioxidants and antimicrobial agents with a high surface area catalytic activity.

Keywords: *Artemisia argyi,* green synthesis, characterization, antioxidant activity, antimicrobial activity

ACKNOWLEDGEMENT

First of all, I would like to express my sincere gratitude to my supervisor, Miss Anto Cordelia Tanislaus Antony Dhanapal for guiding and supporting me with a lot of patience and effort throughout this research.

Besides, I would like to express this appreciation to the university UTAR for providing me an opportunity to complete my final year project with the sufficient facilities and equipments. I would also thank laboratory officers and postgraduates in UTAR which guided me in the operation and utilization of the equipments and also for their sharing of knowledge in this research.

Last but not least, I would like to thank my family and friends for their moral support throughout this research.

DECLARATION

I hereby declare that the project report is based on my original work except for quotations and citations which have been dully acknowledged. I also declare that is has not been previously or concurrently submitted for any other degree at UTAR or other institutions.

<div align="right">

_____

HNG HUEY PING

</div>

This project report entitled "**INVESTIGATION OF GREEN SYNTHESIZED SILVER NANOAPRTICLES USING AQUEOUS LEAF EXTRACT OF *ARTEMISIA ARGYI* FOR ANTIOXIDANT AND ANTIMICROBIAL POTENTIALS**" was prepared by HNG HUEY PING and submitted as partial fulfillment of the requirements for the degree of Bachelor of Science (Hons) Biochemistry at Universiti Tunku Abdul Rahman.

Approved by:

_____

(Ms. Anto Cordelia Tanislaus Antony Dhanapal)

Date: _____

Supervisor

Department of Chemical Science

Faculty of Science

Universiti Tunku Abdul Rahman

FACULTY OF SCIENCE

UNIVERSITI TUNKU ABDUL RAHMAN

Date: _____

PERMISSION SHEET

It is hereby certified **HNG HUEY PING** (ID No: **13ADB01906**) has completed this final year project entitled "**INVESTIGATION OF GREEN SYNTHESIZED SILVER NANOAPRTICLES USING AQUEOUS LEAF EXTRACT OF *ARTEMISIA ARGYI* FOR ANTIOXIDANT AND ANTIMICROBIAL POTENTIALS**" supervised by Ms. Anto Cordelia Tanislaus Antony Dhanapal from the Department of Chemical Science, Faculty of Science.

I hereby give permission to the University to upload the softcopy of my final year project in pdf format into the UTAR Institutional Repository, which may be made accessible to the UTAR community and public.

Yours truly,

_____
(HNG HUEY PING)

TABLE OF CONTENTS

LIST OF TABLES

LIST OF FIGURES

LIST OF ABBREVIATIONS

ABTS	2,2'-Azino-bis(3-ethylbenzothiazoline-6-sulphonic acid)
Ag	Silver
Ag^+	Charged Silver Atom
Ag^0	Uncharged Silver Atom
$AgNO_3$	Silver Nitrate
AgNPs	Silver Nanoparticles
BDE	Bond Dissociation Energy
C15	Carbon 15
DLS	Dynamic Light Scattering
DPPH	2, 2-Diphenyl-1-picrylhydrazyl
EC_{50}	Half Maximal Effective Concentration
EDAX	Energy Dispersive Spectroscopy
EDTA	Ethylenediaminetetraacetic Acid
$FeCI_3.6H_2O$	Ferric Chloride Hexahydrate
$FeSO_4.7H_2O$	Ferrous Sulfate
FESEM	Field Emission Scanning Electron Microscope
FRAP	Ferric Reducing Antioxidant Power
FTIR	Fourier Transform Infrared
GAE	Gallic Acid Equivalent
HAT	Hydrogen Atom Transfer
IPE	Ionization Potential Energy
KBr	Potassium Bromide
K_2HPO_4	Dipotassium Hydrogen Phosphate

KH_2PO_4	Potassium Dihydrogen Phosphate
$K_2S_2O_8$	Potassium Persulfate
NMR	Nuclear Magnetic Resonance
NNI	National Nanotechnology Initiative
NO	Nitric Oxide
OD	Optical Density
O-H	hydroxyl group
PBS	Phosphate Buffer Saline
QE	Quercetin Equivalent
ROS	Reactive Oxygen Species
SEM	Standard Error Mean
SET	Single Electron Transfer
SRP	Surface Plasmon Resonance
TCN	Tetracycline
TFC	Total Flavonoid Content
TPC	Total Phenolic Content
TPTZ	2,4,6-Tripyridyl-s-triazine
UV-Vis	Ultraviolet Visible
XRD	X-Ray Diffraction

CHAPTER 1

INTRODUCTION

Nanotechnology is a big scale of nanometer size particles manufacturing, especially on metal based nanoparticles only of those between 1 to 100 nm in size (NNI, 2000; Hulla, Sahu and Hayes, 2015). The nanotechnology or nanoscience has been well known for some time. In 2000, United States National Nanotechnology Initiative (NNI) stands as worldwide pace for the nanotechnology projects. From the information in National Nanotechnology Initiative, it was first started by a physicist, the father of the nanotechnology known as Richard Feynman at 1959 on December 29 which explained his concept on the manipulation of atoms and molecules. The fundamental of nanoscale research was therefore based on a concept on which how the atoms or molecules could be controlled or manipulated. This was followed by Professor Norio Taniguchi which created the term 'Nanotechnology' in his book entitled, "Engines of Creation" at 1986 in describing the semiconductor processes at nanometer level. The research on nanotechnology projects contributes largely in nanoscale electronic, optics, energy, environmental remediation and medical applications (NNI, 2000; Hulla, Sahu and Hayes, 2015). The nanotechnology was not only limited to electronic devices in daily life but they have also emerged into food industry and medicinal manufacturing area which uses nanoparticles as coating materials for antiseptic practices (Ahmed, et al., 2016).

Nanotechnology was emerged as a new era in science and technology world when the microscopic instruments were built to enable the observation on the morphology and structure of the nanoscale particles (NNI, 2000). These nanoparticles are of variety shapes and sizes. These properties can be used to control and provide specific or enhanced effects on the applied products (Johnson and Obot, 2014). In optics view, the nanoparticles building from metal supplied a thin layer of electron density medium which enabled the occurrence of surface plasmon resonance that helped in producing strong light scattering and light absorption. Currently, the synthesis of nanoparticles has developed from physical method to chemical method and from chemical method to biological method with the help of natural reducing compounds in living organisms (Iravani, et al., 2014).

1.1 Research Background

After the inconvenience caused by the machines usage in physical method and toxic by-products in chemical synthesis, the biosynthesis using fungi, microbes, algae and plants has been introduced for the more environmental and cost effective production of nanoparticles (Prabhu and Poulose, 2012). Plants used in biosynthesis are of particular interest because it is faster and does not require selection from many species as in other living organisms. Currently, many extract from plants have been proven to possess the ability to reduce and stabilize the nanoparticles and this process is particularly known as green synthesis (Iravani, et al., 2014). Among the metal nanoparticles, silver nanoparticles were of interest in medical field as it was claimed to possess potential in antimicrobial activity against Gram positive and Gram negative

bacteria (Abdel-Aziz, et al., 2014). Studies also showed that the synthesis processes are affected by synthesis conditions which affect the outcome of nanoparticles (Mansouri and Ghader, 2009; Ahmed, et al., 2016). A few studies reported that the antioxidant activity caused by the binding of phytochemicals from plants onto the surface of nanoparticles has been enhanced in comparison to the plant extract alone (Abdel-Aziz, et al., 2014; Patra and Baek, 2016; Phull, et al., 2016). A few types of *Artemisia* plants have been studied to produce mostly spherical silver nanoparticles. Sunlight irradiation has also been used recently and proven the ability to induce the reduction process in the *Artemisia* plant (Johnson and Obot, 2014). Therefore, *Artemisia argyi* is selected for green synthesizing of silver nanoparticles through sunlight irradiation which may be a potential source of spherical shape nanoparticles, effective antioxidant agents and antimicrobial agents.

1.2 Research Rationale

Data on green synthesis of silver nanoparticles using *Artemisia argyi* is limited and none has been reported in Malaysia. The explanation on the synthesis using higher concentration of silver source and properties of the silver nanoparticles synthesized using this plant under influence of sunlight in local area is also insufficient. Hence, the current study was undertaken to characterize and evaluate the antioxidant and antimicrobial potentials of the silver nanoparticles synthesized using *Artemisia argyi* as the environmental friendly and cost effective method.

1.3 Research Objectives

The aim of this research is to evaluate the properties of silver nanoparticles synthesized using *Artemisia argyi* through characterization, antioxidant and antimicrobial studies.

Below are the specific objectives of this research:

1) To synthesize silver nanoparticles from silver salts using *Artemisia argyi* aqueous extract by sunlight irradiation.

2) To characterize silver nanoparticles synthesized using *Artemisia argyi* into their morphology, sizes and structure using UV-Vis, FESEM, FTIR and XRD analysis.

3) To study the effect of silver salts concentration in synthesizing silver nanoparticles.

4) To study the antioxidant activity of silver nanoparticles using free radicals scavenging assays and ferric reducing assay.

5) To evaluate antimicrobial activity of silver nanoparticles using Gram negative *Escherichia coli* and Gram positive bacteria *Staphylococcus aureus*.

CHAPTER 2

Literature review

2.1 Review of Silver Nanoparticles

2.1.1 Background

Silver nanoparticles (AgNPs) are nanoscale particles made up from atomic silver (Ag). Besides being known as silver nanoparticles, they can be referred as nanoparticles of silver, nanoscale silver or nanosilver. Their relatively large surface area to their volume contributes to an enhancement in carrying out reaction which has been partaken in the medical application. They can be synthesized by physical, chemical and biological method from metallic silver or ionic silver size (Khouloud, et al., 2010). In fact, different source of reducers and conditions are the main contributor to their characteristics in term of sizes, shapes, morphology and structures (Mansouri and Ghader, 2009). Silver nanoparticles can be categorized into different shapes such as nanowires, nanocubic, nanospheres, nanorods, nanobar, nanotriangular, nanoprisms, nanowedges or the combination of different shapes in one silver nanoparticles (Pyatenko, Yamaguchi and Suzuki, 2007; Wiley, et al., 2007; Chang, Lu and Chou, 2011; Pourjavadi and Soleyman, 2011; Kelly, Keegan and Brennan-Fournet, 2012; Kou and Varma, 2013; Poinern, et al., 2013). Silver nanoparticles are well known for its good potential in antimicrobial activity as they can effectively inhibit the growth of pathogenic bacteria (Khouloud, et al., 2010; Prabhu and Poulose, 2012). They contributed mainly in medical applications which focus on aseptic practices. They are microscopic particles

which ranging from 1 to 100 nanometer in size (Khouloud, et al., 2010). Besides, metal nanoparticles including silver nanoparticles have a unique surface property known as surface plasmon resonance (SRP) which resulted from the incident light that excites the electron density on the surface of the metal thin layer film (Smitha, et al., 2008; Mahmudin, et al., 2015). The resonant effect of silver nanoparticles was also claimed to be dependent on the size and shape distribution in the nanoparticles which could cause a shift in color appearance or wavelength of light (El-Brolossy, et al., 2008).

2.1.2 Chemistry of Silver Element (Ag)

 Silver (Ag) is a transition metal with a face centered cubic crystalline structure (Greenwood and Earnshaw, 1997). Some common use of Ag involves the making of Ag based electronic equipments and glasses in accordance to their high thermal and electrical conductivity than other metals (Drake and Hazelwood, 2005). The Ag in ionic form from soluble compounds usually absorb at UV- region around 200 nm to 400 nm as shown in previous study on spectral of Ag ions due to the electron in the filled d band (Abdelghany, ElBatal and ElBatal, 2015). For decades, Ag had been extensively used as antimicrobial agents in medical field to protect against microbial infections (Alexander, 2009). The medical instruments that are made up from Ag coatings are more likely to prevent infection during surgery processes and patient treatment. Silver nitrate ($AgNO_3$) is inorganic Ag compound which is formed by reaction of Ag in nitric acid with lower light sensitivity. When dissolve in solvent such as water, $AgNO_3$ deionizes into Ag ions and nitrate ions. The Ag ions in the soluble form can be used as strong

antimicrobial agent against pathogenic bacteria. In general, Ag ions disrupt the bacteria cell membrane followed by invasion and affecting the normal cell function which causes the inhibition of the cell replication and protein synthesis (Cason, et al., 1966; Chopra, 2007; Jung, et al., 2008). Meanwhile, the toxicity of Ag have been claimed to cause argyria and argyrosis only in its soluble form (Drake and Hazelwood, 2005).

2.1.3 Agglomeration of Nanoparticles

Metal nanoparticles including silver nanoparticles are relatively prompt to agglomeration under the absence of a protective capping agent. Agglomeration is an irreversible aggregation of fine particles that takes place in order to overcome the instability caused due to high surface energy and coordination unsaturation induced by large surface area of nanometer-sized particles (Li, Lin and Zhao, 2002). A capping agent protects them from agglomeration by forming a layer of protective film on the surface of nanoparticles (Kholoud, et al., 2010). Previously, the protective layers are supplied by synthetic chemicals such as poly (ethylene glycol) (PEG), poly (vinyl alcohol) (PVA), poly methacrylic acid (PMA) and poly (vinylpyrrolidone) (PVP) and now switches to a more environmental friendly biocapping agents from living organisms (Iravani, et al., 2014).

2.1.3   Importance of Silver Nanoparticles in Medical Field

The study of silver nanoparticles is important for their antimicrobial activity against various pathogenic bacteria as to assist in the development of cleanliness practices in medical manufacturing around the world. Silver

nanoparticles have been successfully synthesized through green synthesis utilizing naturally occurring plant extracts and fungus which were reported to possess effective inhibition effect on the growth of pathogenic bacteria (Araújo, et al., 2012;Vankar and Shukla, 2012; Maiti, et al., 2014; Hseuh, et al., 2015). They also contribute in the sanitization of utensils in which they have been reported to effectively kill bacteria which adhere to stainless steel (Araújo, et al., 2012). Due to its antimicrobial property, they are also used in water purification process in order to remove water-borne viruses and health threatening microorganisms (Zhang, 2013). Besides as antimicrobial agent, they are effective anticancer agents too. Such cases can be seen in silver nanoparticles synthesized from *Spinacia oleracea* aqueous extract and *Syzygium aromaticum* which have been reported to possess excellent antiviral abilities against cancer cells of mouse myoblast, breast and lung (Ramachandran, et al., 2017; Venugopal, et al., 2017). They are claimed to inactivate virus infection through the binding to the virus receptor (Ge, et al, 2014). They are also reported as potential antioxidant agents caused by the antioxidants compounds adsorbed to the surface of green synthesized silver nanoparticles which could help to scavenge commercially known free radicals such as DPPH, hydroxyl radicals, hydrogen peroxide, iron metal ions and nitric oxide (Giridharan, et al., 2014). Besides, they were also claimed to possess anti-inflammatory effects (Krithika, et al., 2016; Sakthivel and Anitha, 2016). Therefore, it is crucial to investigate the use of silver nanoparticles in assisting the medical manufacturing and disease treatment.

2.2   Synthesis of Nanoscale Particles

2.2.1 Top- Bottom and Bottom-Top Approaches

The synthesizing methods for nanoparticles such as top - bottom and bottom - top approaches are subdivided into physical, chemical and biosynthesis (Iravani, et al., 2014). The top to bottom approach is described by the formation of nanoparticles from a larger metal material through the evaporation condensation of the metal source into fine nanoscale particles, an approach used in physical synthesis of nanoparticles (Ahmed, et al., 2015). Meanwhile, bottom to top is achieved through the arrangement of metal atoms from silver based compounds such as silver halides and silver nitrate into a group of well distributed particles, usually in a solution form aided by reducing agents, are mainly applied in the chemically and biologically synthesis of nanoparticles (Wang and Xia, 2004). The main differences between physically, chemically and biologically synthesis of silver nanoparticles are in term of force applied to the metal sources, presence of toxic or non-toxic reducing agents and the physical state of the nanoparticles (Gudikandula and Maringanti, 2016).

2.2.2 Physical Synthesis

Evaporation-condensation and laser ablation are commonly used in physical synthesis approach of nanometer-sized of silver particles (Iravani, et al., 2014). Two important features of physical approach are: they are chemical free and they involve synthesis of fine nanoparticles from a metal source. Both techniques utilize the high metal shearing forces such as high temperature in the tube furnace and laser irradiation (Machmudah, et al., 2013). Due to time

demanding, space occupying and high energy consumption synthesis process in the physical method, it was taken over by the chemical synthesis (Khouloud, et al., 2010).

2.2.3 Chemical Synthesis

Chemical synthesis is a bottom to top approach where a group of atoms or molecules arranges themselves into nanoparticles. In order to chemically synthesize silver nanoparticles, the synthetic reducing compounds are used to reduce silver ions (Ag^+) into uncharged silver atoms (Ag^0) followed by rearrangement into silver nanoparticles (Iravani, et al., 2014). The synthetic reductants are used for the synthesis of nanoparticles which includes monosaccharides of sugar, citrate and borohydride of sodium and other reagents such as poly (ethylene glycol) (PEG), ascorbate, hydrogen element, N,N-dimethyl formamide (DMF) and Tollen's reagent (Tran, Nyugen and Le, 2013; Ahmed, et al., 2015). However, the nanoparticles produced are so unstable with tendency to agglomerate that they require synthetic stabilizing agents to form a protective layer on each of the particles (Kheybari, et al., 2010; Guzmán, Dille and Godet, 2008). The drawback of utilizing the chemical reducers is that they require an additional synthetic stabilizer to prevent them from agglomeration and secondly, the undesirable generation of toxic by-products due to the utilization of synthetic reducing agents, posting harmful effect on the environment (Wang, et al., 2005; Prabhu and Poulose, 2012; Iravani, et al., 2014). Again, the safety of nanoparticles produced using chemical agents of concern and more environmental friendly way of

producing silver nanoparticles by biologically-based method has been introduced.

2.2.4 Biosynthesis

Biosynthesis of silver nanoparticles is a bottom to top method that is advantageous over chemically synthesized silver nanoparticles due to its simplicity, toxic-free and stability from agglomeration (Ahmed, et al., 2015; Gudikandula and Maringanti, 2016). In biosynthesis, silver nanoparticles is produced in a way that the reduction process is similar to chemical synthesize but with the utilization of naturally occurring reducers such as reducing compounds extracted from plant, bacteria, algae or fungi (Prabhu and Poulose, 2012, Velusamy, et al., 2016). Moreover, the presence of phytochemicals in plants was claimed to help in coating the surface of the nanoparticles as capping agent to prevent agglomeration (Tran, Nyugen and Le, 2013; Iravani, et al., 2014; Ahmed, et al., 2015). They are capable in reducing Ag^+ into silver nanoparticles due to their reducing power in the phytochemicals such as phenolic compounds (Prabhu and Poulose, 2012). As the content and nature of phytochemicals in plants are different, they will synthesize silver nanoparticles of varieties. Moreover, the green synthesized silver nanoparticles were also been reported to possess rich antioxidant polyphenols compounds (Bhakya, et al., 2016; Mahendran and Kumari, 2016; Patra and Baek, 2016; Salehi, et al., 2016). Therefore, the antioxidant study of green synthesized silver nanoparticles using plant extracts can be further established.

2.2.5 Mechanism in Bottom – Top Approaches

The synthesis of nanoparticles proceeds via three main stages as proposed by Makarov, et al. (2014). This includes the activation, growth and termination stages. In the activation stage, metal ions are reduced into uncharged metal atoms ($Ag^+ + e = Ag^0$) followed by nucleation of these metal atoms into crystal structure (Vetter, et al., 2013). During the growth stage, the metal nanoparticles crystals will assemble and grow into larger particles through Ostwald ripening with the rise in the thermodynamic stability. This was also in agreement with mathematical calculation by Liu, et al. (2007) in the Ostwald Ripening of β-Carotene Nanoparticles. The morphological characteristics of the nanoparticles are then determined during the termination stage. The nanoparticles arrange themselves into the most stable conformation to overcome the high surface energy such as forming truncated structure (Kim, et al., 2010). However, under the presence of stabilizing agents from plants in the termination phase, the truncated structure can be prevented and the less stable structure can be supported (Makarov, et al., 2014). Overall, the silver nanoparticles is synthesized via crystal growth mechanism.
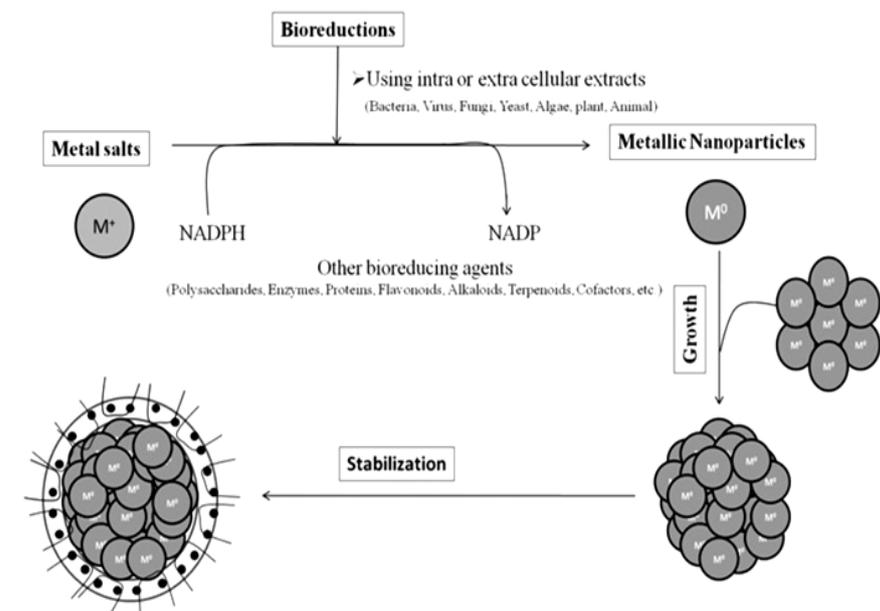
Figure 2.1: Mechanism of silver nanoparticles synthesis.

2.2.6 Influence from Silver Nanoparticles Synthesizing Conditions

The green synthesis of silver nanoparticles is also affected by several aspects such as pH, concentration of chemicals, incubation period, temperature and phytochemicals from plant extracts (Mansouri and Ghader, 2009; Makarov, et al., 2014; Velusamy, et al., 2016). The pH environment should be compatible with the metal binding capacity of functional groups from extracts. The suitable pH allows the proper interaction between the functional group from reducing agents and silver ions in the synthesis of silver nanoparticles. In contrast, when plant extracts and silver ions are reacted in incompatible pH environment, the interaction is distorted and will cause an unfavorable outcome such as agglomeration of nanoparticles (Makarov, et al., 2014; Ibrahim, 2015). Meanwhile, temperature is also a great factor that contributes to the formation rate and morphology of silver nanoparticles synthesis. Rise in temperature causes the rise in reaction rate and the rate efficiency of

nanoparticles formation, thereby increasing the nucleation rate (Amin, et al., 2012; Makarov, et al., 2014; Ibrahim, 2015). The amount of silver nanoparticles can also be controlled by the concentration of silver salts and reducing compounds such that the increasing of these sources promote the synthesizing of silver nanoparticles as proven in previous studies (Ahmed, et al., 2016).

2.2.7 Plant Extraction Technique

In green synthesis of silver nanoparticles, the plant extracts were mostly prepared by boiling the plant in aqueous solution such as deionized water as this method is simple and non-toxic (Hussain, et al., 2014; Anandalakshmi, Venugobal and Ramasamy, 2015). Boiling method was frequently used in preparing the plant extracts because higher temperature treatment helps to extract some thermal stable compounds such as phenolic and flavonoids at a higher efficiency as reported in previous studies (Wan, et al., 2011; Amadou, Le and Shi. 2012; Godlewska, et al., 2016). The use of boiling in phenolic compounds extraction was also proven to increase the extract of phenolic compounds and the subsequent antioxidant activity of some plant species in earlier studies (Ogunmoyole, et al., 2012; Sharma, et al., 2015; Godlewska, et al., 2016).

2.3 Characterization of Silver Nanoparticles

The evaluation of synthesized silver nanoparticles on their morphology and structure are important as they associate with the understanding of the synthesis process, compounds involved and the structural information of

synthesized silver nanoparticles. This can be affected by several factors such as pH, time, components and concentration of chemical, electrical potential of metal ions and temperature. Silver nanoparticles can be categorized based on their absorption peak, morphology along with other features such as functional groups, crystalline properties, elements content, zeta potential charge and size distribution through the assistance from various instruments such as microscopes, spectrophotometers, infrared spectroscopy, X-ray diffractometer, EDAX, NMR spectroscopy and DLS (Khouloud, et al., 2010).

2.4 Background of *Artemisia argyi*

2.4.1 Origin of *Artemisia argyi* and Its Traditional Medicinal Function

The medicine values of Chinese mugwort (*Artemisia argyi*) have been widely spread around the world. *Artemisia argyi* is one of the well known medicinal mugwort in China (Adams, Garcia and Garg, 2012). It is also known as Chinese mugwort, located and transported over Asia countries. It is from the genus of *Artemisia* and in the family of Asteraceae. The origin of *Artemisia argyi* was recorded in the Compendium of Materia Medica which attributes its origin to that Tangyin county in China (Huang and Qiu, 2014). *Artemisia argyi* is used in stimulating blood flow during moxibustion as moxa leaf (Adams, Garcia and Garg, 2012). An Australian acupuncturist in her publication of *Moxa Use in Pregnancy* stated that the moxibustion using moxa leaf releases the tension in the mother's body therefore solving the problem of incorrect position of fetus in the mother's womb (Bruce, 2012).

2.4.2 Phytochemicals Content in *Artemisia argyi*

In addition to its traditional medicine values in moxibustion and pregnancy, in modern science, many studies conducted in Asia countries such as China and Korea on the aqueous extract of *Artemisia argyi* showed that number of bioactive compounds were detected which includes flavonoids, essential oil, polysaccharides, monoterpene, lactones, phenolic glycoside, chromone and phenolic acid which allow the *Artemisia argyi* to possess strong antioxidant capacity against various harmful radicals and some possessed immunity promoting activity (Wu and Sun, 2008; Huang, et al., 2012; Chu, et al., 2015; Zhang, et al., 2016; Zhao, et al., 2016). While majority studies of *Artemisia argyi* was conducted in China, the study of *Artemisia argyi* in local Malaysia is limited. From a local study, the phytochemical screening of local *Artemisia argyi* showed that it contains large quantities of polyphenol compounds such as flavonoid and phenolic compounds which possessed a good reducing power on metal ions (Anto Cordelia, et al., 2016).

Secondary metabolites	Aqueous extract	Ethanolic extract	Methanolic extract
Alkaloid	-	-	-
Antraquinone	-	-	-
Flavonoid	+	+	+
Phlobatannin	-	-	-
Saponin	+	+	+
Steroid	-	+	+
Tannin	-	+	+
Terpenoid	-	-	-
Essential oil	-	+	+

(+) Presence of phytochemical compounds. (-) Absence of phytochemical compounds.

(Source: Anto Cordelia, et al., 2016)

Figure 2.2: Phytochemical constituents of local *Artemisia argyi* crude extract.

2.4.3 Antioxidant Capacity of Local *Artemisia argyi*

The antioxidant activity of local *Artemisia argyi* plant extract has been conducted in previous study by Anto Cordelia, et al. (2016). They reported that the plant extract of local *Artemisia argyi* contains high phenolic and flavonoid content. Moreover, the antioxidant activity assays have been evaluated using radical scavenging assays (ABTS, DPPH, NO), iron chelation and reducing power (FRAP) and showed that aqueous extract contain a higher iron chelating activity. The information for the antioxidant activity of the plant extract originated from Kampar will be useful as a comparison in this research to investigate the antioxidant capacity of the silver nanoparticles synthesized using the plant of same origin. The reported antioxidant content of phenolic and flavonoid with the antioxidant capacity of the plant extract are shown as below:

Bioactive compounds	*Artemisia argyi* extracts		
	Aqueous	Ethanolic	Methanolic
Total phenolics (mg GAE/g dry matter)	68.87 ± 0.70	80.53 ± 2.66	234.52 ± 0.99
Total flavonoids (mg QE/ g dry matter)	83.37 ± 31.88	449.81 ± 5.59	737.72 ± 25.55

GAE, gallic acid equivalents; QE, quercetin equivalents, values reports as mean ± standard errors (n=3)

Leaf extract of *Artemisia argyi* or Standard	Iron chelating activity assay EC_{50}**	DPPH radical scavenging assay EC_{50}*	NO scavenging assay EC_{50}**	ABTS radical cation scavenging assay		FRAP assay	
				EC_{50}**	TEAC***	FRAP values****
Aqueous extract	3.05 ± 0.07	105.73 ± 6.72	2.34 ± 0.06	0.20 ± 0.00	1.07 ± 0.04	0.39 ± 0.01
Ethanolic extract	4.21 ± 0.15	107.95 ± 1.32	1.05 ± 0.01	0.20 ± 0.01	1.07 ± 0.06	0.68 ± 0.00
Methanolic extract	4.20 ± 0.15	63.34 ± 1.10	0.96 ± 0.01	0.11 ± 0.01	1.95 ± 0.24	2.38 ± 0.06
Ascorbic acid	-	6.55 ± 0.10	0.27 ± 0.00	-	-	-
EDTA	0.023 ± 0.001	-	-	-	-	-

* µg/mL; ** mg/mL; *** mmole Trolox equivalents/ g dry matter; **** mmole Fe2+ equivalents / g dry matter

(Source: Anto Cordelia, et al., 2016)

Figure 2.3: Investigation of antioxidant activity in local *Artemisia argyi*.

2.5 Potential of Local *Artemisia argyi* in Nanosynthesis of Silver

The research of local *Artemisia argyi* on its ability to synthesize silver nanoparticles is limited in Malaysia. On the other hand, studies on another species of mugwort such as *Artemisia marschalliana* by Salehi, et al. (2016) at Iran in the *International Journal of Nanomedicine* reported that spherical shape of silver nanoparticles are formed with size ranging from 5 nm to 50 nm. The presence of bioactive compounds in the nanoparticles was screened and found that they successfully inhibited cancer cells by downregulating anti apoptosis *Bcl-2* gene. The silver nanoparticles from *Artemisia marchalliana* was also capable of scavenging DPPH radicals and exhibited stronger inhibitory effects against Gram- negative bacteria *by a suggested silver ions membrane-damaging mechanism* (Salehi, et al., 2016). Meanwhile, other species of *Artemisia* that have been studied includes *Artemisia annua, Artemisia nilagirica, Artemisia capillaris, Artemisia absinthium* and *Artemisia vulgaris* which is centered on the antibacterial activity in silver nanoparticles (Vijayakumar, et al., 2013; Giri, et al., 2014; Johnson and Obot, 2014; Jang, et al., 2015; Ali, et al., 2016). Furthermore, the shapes of silver nanoparticles synthesized from these *Artemisia* species were reported to be mostly in spherical. Besides, the local *Artemisia argyi* extract has been found to possess remarkable content of flavonoid and phenolic compounds in its polar extracts (Anto Cordelia, et al., 2016). These reducing compounds in *Artemisia argyi* are particularly potential towards the synthesis of silver nanoparticles. The studies of *Artemisia argyi* were mostly concentrated on the chemical constituents and antioxidant activity of its extracts. The local *Artemisia argyi* may have better reducing and stabilizing ability. Therefore, further

investigation on the characterizations, antioxidant capacity, and antimicrobial activity on the silver nanoparticles synthesized using local *Artemisia argyi* was initiated.

2.6 Antioxidant Activity in Antioxidant Compounds

2.6.1 Free Radicals and Oxidative Stress

Free radicals are uncharged molecules that have at least one unpaired electron in their orbital (Lobo, et al., 2010). In living organism, free radicals such as reactive oxygen species (ROS) and reactive nitrogen species (RNS) are formed as natural byproducts during the cellular metabolism which are relatively high reactive and are unstable (Dröge, 2002). In the case of ROS, the molecular oxygen undergoes sequential reduction which forms free radicals such as peroxide, superoxide anion, singlet oxygen and hydroxyl radicals (Valko, et al., 2007). The process when reactive species produced in excess attack the nearby stable molecules in order to stabilize themselves causing harmful effects to the organic molecules in the body known as oxidative stress (Pham-Huy, He and Pham-Huy, 2008). The destabilization of neighbouring molecules caused by the electron stealing free radicals usually result in a chain series attack of reactive species. A few diseases have been documented to have correlations with the oxidative damage resulted from free radicals' attacks such as cancer, cardiovascular, neurological, pulmonary, nephropathy, ocular and rheumatoid arthritis diseases thereby suggesting the needs to overcome the damage caused by free radicals (Young and Woodside, 2001).

2.6.2 Antioxidant Defense System

To overcome oxidative stress, living organisms utilize antioxidant defense system to terminate the damage from reactive free radicals by donating or accepting electrons (Gupta and Sharma, 2006). The two main pathways are enzymatic pathway and non-enzymatic pathway (Dröge, 2002). The enzymes involved in the antioxidant defense system include catalase, superoxide dismutase, glutathione peroxidase and reductase which help in converting harmful radicals into water and oxygen. In non-enzymatic pathway, besides metabolic antioxidants which can be synthesized in the body, exogenous antioxidants (nutrient antioxidant) are radical scavenging compounds which need to be obtained through diets (Pham-Huy, He and Pham-Huy, 2008). The exogenous antioxidants are particularly essential in scavenging free radicals when the host defense system is down regulated or when overproduction of free radicals in the system cannot be overcome. Interestingly, plants are acting as a universal source for nutrient antioxidant supply such as Vitamin E, Vitamin C, carotenoids, flavonoids, trace metals and omega fatty acids (Gupta and Sharma, 2006; Kasote, et al., 2015).

2.6.3 Antioxidant Compounds in Plant

In plants, polyphenol compounds are secondary metabolites which defend the system against environmental stress. They are divided into few classes such as phenolic acids, stillbenes, flavonoids and lignin and lignans (Spencer, et al., 2008). Polyphenols are potential antioxidant compounds and were claimed to possess radical scavenging activities (Alfadda and Sallam, 2012). The scavenging of polyphenol proceeds via transferring of hydrogen atom (HAT)

and electron transfer (ET) (Huang, Ou and Prior, 2005). In hydrogen transferring, presence of free radicals induces transfer of hydrogen from phenol OH bond, ArOH to the free radicals forming RH and ArO* respectively where the reaction relies on the dissociation energy of phenolic bond (BDE) (Bendary, et al., 2013). On the other hand, ET pathway involves the transfer an electron from antioxidants to the free radicals resulted in formation of R^- and $ArOH^{*+}$ instead of losing hydrogen atom as in HAT where the reaction relies on the ionization potential (IP) (Zhuravlev, 2016). The lower BDE and IP values always lead to higher free radicals scavenging activity because when the energy required for dissociation of O-H bond lowers, the bond dissociates easily to donate the hydrogen atom. Also, when the IP decreases, the energy needed to remove the electrons from antioxidants is lowered and therefore facilitated the transfer of electrons to the free radicals (Wright, Johnson and Di Labio, 2001). Besides scavenging radicals, polyphenols in plant are also able to chelate metal ions through transition metal chelation to prevent the generation of ROS in the presence of hydrogen peroxide (Anto Cordelia, et al., 2016).

Flavonoids are important antioxidant compounds. They are polyphenol compounds with C15 skeleton sharing the basic structure C6-C3-C6 (Ghasemzadeh and Ghasemzadeh, 2011; Mlcek, et al., 2016). They can be grouped into flavones, flavanols, isoflavones, flavonols, flavanones and anthocyanins (Pandey and Rizvi, 2009). Many plants are claimed to contain flavonoids which possess a strong antioxidant activity besides reported to contain anti-inflammatory, antimicrobial, antihistamine, anticancer, anti-

allergic and antinociceptive activity in many studies (Mlcek, et al, 2016; Chen, et al., 2016; Ravishankar, et al., 2013; Kawai, et al, 2007).

While plants contain polyphenol compounds, they are claimed to 'pass down' these essential bioactive compounds to their synthesized products, silver nanoparticles during the reduction of silver ions (Abdel-Aziz, et al., 2014). Phytochemicals from plants attached to the silver nanoparticles surface, act not only as capping agents but also to provide them with antioxidant capacity in scavenging reactive radicals. The presence of bioactive compounds from plant extract have been determined by the detection of functional groups in silver nanoparticles including hydroxyl group, carbonyl groups and amide groups from plants (Patil, Rajiz and Sivaraj, 2015; Bhakya, et al., 2016). Silver nanoparticles are therefore possessed the antioxidant ability to scavenge radicals as they can donate and accept electrons to stabilize the radicals with the presence of these polyphenol compounds attaching on their surface (Bhakya, et al., 2016).

2.7 Principles of Antioxidant Assay

2.7.1 2,2'-azino-bis(3-ethylbenzothiazoline-6-sulphonic acid (ABTS) Radical Scavenging Antioxidant Assay

In ABTS radical scavenging assay, the scavenging capacity was indicated by the decolorization of dark blue $ABTS^-$ radicals. The $ABTS^-$ radicals were first prepared by the persulfate oxidation of colorless reduced $ABTS^{2-}$. The colored $ABTS^-$ radicals will then undergo reduction by the antioxidant compounds back into the colorless $ABTS^{2-}$ therefore resulting in decolorization of the

solution (Shalaby and Shanab, 2012). The ABTS radicals are highly degradable and decompose over time. These colored ABTS⁻ radicals can be detected colorimetrically by light absorption at 734 nm (Shalaby and Shanab, 2012; Huang, Ou and Prior, 2005).

2.7.2 2,2-diphenyl-1-picrylhydrazyl (DPPH) Radical Scavenging Antioxidant Assay

DPPH are synthetic free radicals which are commercially used due to its good stability characteristic (Irshad, et al., 2012). From its chemical structure as shown, the radical site is embedded between the bulky ring chemical groups. In the DPPH antioxidant assay, the purple colored DPPH radicals can undergo reduction through the transfer of hydrogen atom from antioxidants into the radical site to form the yellow reduced product known as a-diphenyl- beta-picrylhydrazine (Salehi, et al., 2016). The DPPH radicals are measured colorimetrically at 515 nm wavelength of light for the determination of antioxidant activity in the antioxidant compounds (Shalaby and Shanab 2012).
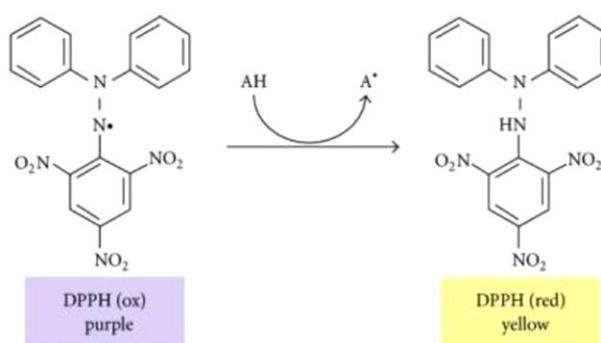
(Source: Texeira, et al., 2013)

Figure 2.4: DPPH radical scavenging activity assay principle.

2.7.3 Iron Chelating Activity

Transition metal ions are used in the body system as part of enzymes or complexes. However, these ions can induce lipid oxidation resulting in the oxidative damage when elevated (Anto Cordelia, et al., 2016). In the assay, purple ferrous ferrozine ions was formed from ferrous ions and ferrozine compound which can be read at 562 nm and the iron chelating acitivity can be determined by the decolorization of purple color due to formation of the Fe-antioxidant complex (Adjimari and Asare, 2015).

2.7.4 Reducing Power

The principle of ferric reducing antioxidant power (FRAP) assay relies on the formation of ferrous ions (Fe^{2+}) from the reduction of ferric ions (Fe^{3+}). As the ferric and ferrous ion are both colorless, the ferric ions form complex with the triazine reagent under acidic condition in order to maintain their solubility and the electron transferring process to form colorless, Fe^{3+} tripyridyltriazine which can be reduced by antioxidants into colored complex, Fe^{2+} tripyridyltriazine (Payne, et al., 2013). The reduced colored complex can be measured colorimetrically by light absorption of these complexes at 593 nm (Sadeghi, et al., 2014).

2.7.5 Nitric Oxide (NO) Scavenging Antioxidant Assay

Nitric oxide (NO) as a part of free radicals in human body system can cause oxidative damage when reacted against superoxide radical to form peroxynitrite anion (Boora, Chirisa and Mukangnyama, 2014). The concentration of nitric oxide can be measured by the formation of pink colored

nitrite ions caused by the NO radicals and O_2 reaction at the physiology pH (Hazra, Biswa and Mandal, 2008). The scavenging activity can be determined from the degree of decolorization in solution at 546 nm (Anto Cordelia, et al., 2016).

2.8 Antimicrobial Mechanism of Silver Nanoparticles

The antimicrobial mechanism of silver nanoparticles was claimed to remain unclear. Two main proposed antimicrobial mechanisms in silver nanoparticles are the damage by free radicals and release of silver ions from silver nanoparticles (Prabhu and Poulose, 2012; Fu, et al., 2015). In the first proposed mechanism, the process starts with the destabilization of membrane permeability and composition of bacteria cell wall by the assembled silver nanoparticles therefore making it more susceptible to extracellular damages (Fu, et al., 2015). The subsequent damage is then overtaken by free radicals induced by the silver nanoparticles - bacteria surface contact which damages the cell membrane and lead to cell death (Prabhu and Poulose, 2012). Meanwhile, the second mechanism suggested that silver nanoparticles release silver ions (Ag^+) which rupture the bacteria cell wall and inactivate enzyme activity by forming conjugations with the amino acids through the thiol groups (Rawashded and Haik, 2009; Hseuh, et al., 2015). Previous studies also reported that the presence of liposaccharides and techoic acid causes the bacteria cell wall to become negatively charged in Gram negative and Gram positive bacteria respectively and facilitated the surface positive charges of the silver nanoparticles to bind to the bacteria cells (Gottenbos, et al., 2001; Feng, et al., 2015).

CHAPTER 3

MATERIAL AND METHODS

3.1 Overview of Research Methodology

```
┌─────────────────────────────────────────────────────────┐
│   Plant selection and authentication: Artemisia argyi     │
└─────────────────────────────────────────────────────────┘
                            ↓
┌─────────────────────────────────────────────────────────┐
│          Aqueous extraction of leaves powder              │
└─────────────────────────────────────────────────────────┘
                            ↓
┌─────────────────────────────────────────────────────────┐
│             Synthesis of silver nanoparticles             │
└─────────────────────────────────────────────────────────┘
```

Characterization
UV-Vis
FESEM
FTIR
XRD

Antimicrobial
activity
E. coli
S. aureus

Total phenolic content
and total flavonoid
content

Antioxidant activity assays
ABTS
DPPH
Iron Chelating
FRAP
NO

```
┌─────────────────────────────────────────────────────────┐
│                      Data collection                      │
└─────────────────────────────────────────────────────────┘
                            ↓
┌─────────────────────────────────────────────────────────┐
│                    Statistical analysis                   │
└─────────────────────────────────────────────────────────┘
                            ↓
┌─────────────────────────────────────────────────────────┐
│                   Result interpretation                   │
└─────────────────────────────────────────────────────────┘
```

3.2 Experimental Procedure

3.2.1 Selection of Plant

Medicinal plant known as *Artemisia argyi* was selected as plant of interest in this project. The morphology and identity of the plant were examined by referring to the related literature (James, et al., 2012; Culiţă and Adrian, 2011). The fresh *Artemisia argyi* leaves were selected and removed from the stem and root.

3.2.2 Preparation of Plant Extract

Fresh leaves were rinsed with running tap water without soaking. The clean leaves were sun dried for subsequent 3 to 5 days and the dried leaves were kept in seal bags for later use. To prepare the leaves extract, the dried leaves were first ground into powder using electric grinder. To prepare 10% *Artemisia argyi* aqueous extract, 25 g of *Artemisia argyi* leaves powder was weighted on weighing scale and was boiled in 250 ml of deionized water for 10 minutes. The boiled extract was left to cool at room temperature for 30 minutes and was vacuum filtered through Whatman filter paper of 70 mm to obtain the aqueous leaf extract of *Artemisia argyi*. The aqueous extract was kept in cool condition at 4 ^{o}C and was used within one week.

3.2.3 Synthesis of Silver Nanoparticles

The preparation of silver nanoparticles from plant extract and silver nitrate was modified from Johnson and Obot (2014). The 0.1 M of silver nitrate (AgNO$_3$) stock solution was prepared by dissolving 1.689 g of AgNO$_3$ solids into 100 ml of deionized water. To prepare 250 ml of 0.01 M of AgNO$_3$

solution, 25 ml of 0.1M AgNO$_3$ stock was measured and added up to a final volume of 250 ml with deionized water. A mixture of aqueous extract and 0.01M AgNO$_3$ in the ratio 1:9 was prepared by mixing 25 ml of aqueous extract in 225 ml of 0.01M AgNO$_3$. The mixture was stirred evenly and placed under direct sunlight for 10 minutes. The color changes were noted. The silver nanoparticles solution was centrifuged at 10,000 rpm for 30 minutes and the supernatant containing impurities was discarded. The pellet was resuspended in deionized water and diluted to 100X. The absorption spectrum of the silver nanoparticles solution was recorded from 300 nm to 800 nm using UV-Vis spectrophotometer (GENESYS 10). The wavelength of the absorption peak was noted. The remaining silver nanoparticles pellet was used for the preparation of the powder.

3.2.4 Preparation of Silver Nanoparticles Powder

Freeze drying method was selected to obtain dried silver nanoparticles powder. The silver nanoparticles pellets from 50 ml silver nanoparticles solution were resuspended in 200 µl of deionized water. The resuspended silver nanoparticles solution was freeze dried overnight using freeze dryer for 16 hours at -45 ^{o}C. The freeze dried silver nanoparticles powder was collected and was kept at 4 ^{o}C for the studies.

3.2.5 Characterization of Silver Nanoparticles

3.2.5.1 UV-Vis Spectrophotometer

Silver nitrate solutions of 0.001 M, 0.005M, 0.01 M and 0.05 M were prepared from silver nitrate stock solution (0.1M). 0.5 ml of 10% *Artemisia argyi* leaves

extract was mixed into 4.5 ml of silver nitrate solution. The mixture was left under projector (5M) for 10 minutes and the absorption spectrum of the solution was recorded from 300 nm to 700 nm wavelength of light using UV-Vis spectrophotometer (GENESYS 10). The results were repeated in triplicates.

3.2.5.2 Field Emission Scanning Electron Microscope (FESEM)

A thin layer of silver nanoparticles powder sample were mounted on the sample holders. The excess powder was removed. The sample was scanned using field emission scanning electron microscope (JEOL USA JSM – 7610F) at magnification of 40,000X. The sample size was analyzed and calculated using ImageJ.

3.2.5.3 Fourier Transform Infrared Spectroscopy (FTIR)

The freeze dried silver nanoparticles were mixed with KBr in 1:10 ratio and the mixture was ground to desired fineness in a mortar. The powder was then pressed in a pump chamber at 4,000 prf to form a KBr disc. The disc was placed in the sample holder and the spectrum was run using FTIR spectrophotometer (Perkin- Elmer). The wavelength of absorbed light was recorded in cm-1. The presence of functional groups was interpreted.

3.2.5.4 X-Ray Diffraction (XRD)

The silver nanoparticles powder sample was prepared. The powder sample was transferred to the XRD holder and the spectrum was run using X-Ray Diffractometer (Siemens D500). The lattice structure, crystalline phase,

crystallite size and purity of silver nanoparticles from *Artemisia argyi* were analyzed using the continuous scan in XRD from 10° to 80° recorded at every 0.02^o interval for 40.0 kV, 30.00 mA and scanning speed of 2.00 degree/min. The wavelength of the X-ray radiation was fixed at 1.54 Ắ.The peaks were observed and compared to the commercial silver database (JCPDS file no 04-0783). The lattice parameters and lattice constant were calculated and tabulated. The crystallite sizes were calculated using Scherrer equation. The secondary phase and presence of impurities were identified.

Scherrer equation

$$D = \frac{K\lambda}{\beta \cos \theta}$$

Where,

D = Crystallite size

K = shape factor (0.9)

λ = wavelength of X-ray (1.54 Ắ)

β = FHWM

3.2.6 Antioxidant Activity of Silver Nanoparticles

3.2.6.1 Total Phenolic Content (TPC)

Total phenolic content in silver nanoparticles was quantified by using Folin Ciocalteu (FC) method from Azlim Almey, et al. (2010). The 1 mg/ml of gallic acid standard was prepared by dissolving 0.01 g gallic acid solids in ethanol and the solution was added up to final volume of 10 ml with deionized water. A working concentration of 0.05, 0.10, 0.15, 0.20 and 0.25 mg/ml of standard gallic acid was prepared by diluting the stock solution with deionized water. The 1mg/ml of silver nanoparticles was prepared by sonicating 0.01 g

silver nanoparticles powder in 10 ml deionized water for 30 minutes using sonication bath. 100 µl of gallic acid or sample was mixed with 750 µl of 10% Folin-Ciocalteu reagent. The mixtures were left at room temperature for 5 minutes. Next, 750 µl of 6 % sodium carbonate (Na_3CO_3) was added into the mixture. The mixture of sample, Folin reagent and sodium carbonate mixture was left at room temperature for 2 hours. Deionized water was used as to blank the spectrophotometer for all the tubes. The absorbance was recorded at 725 nm using UV-Vis spectrophotometer (GENESYS 10). The test was repeated in triplicates and the total phenolic content of silver nanoparticles sample was expressed in gallic acid equivalent ± standard error.

3.2.6.2 Total Flavonoid Content (TFC)

Total flavonoid content in silver nanoparticles was quantified by using method modified from Anto Cordelia, et al. (2016). Quercetin hydrate was used as standard in total flavonoid assay. The 10 ml of 1 mg/ml of quercetin hydrate stock solution was prepared by dissolving 0.01 g of quercetin hydrate solids in methanol. A working concentration for standard was prepared by diluting quercetin hydrate stock to 0.2 mg/ml - 1.0 mg/ml in methanol solution. 1 mg/ml of silver nanoparticles solution was prepared. 150 µl of 5 % sodium nitrite ($NaNO_2$) was added into 200 µl sample and the mixture was left at room temperature for 6 minutes. Next, 150 µl of 10% aluminium chloride ($AlCI_3$) was added into each tubes and the tubes was left again at room temperature for 6 minutes. Lastly, 800 µl of 10% sodium hydroxide (NaOH) solution was added into the mixture. The mixture was left for 15 minutes at room temperature and the absorbance readings were taken at 510 nm using

UV-Vis spectrophotometer (GENESYS 10). The triplicates of the data were obtained and the TFC was expressed in quercetin hydrate equivalent $\pm$ standard error.

3.2.6.3 Silver Nanoparticles Stock Solution

1 mg/ml of silver nanoparticles stock solution was prepared by dispersing 0.05 g of silver nanoparticles in 50 ml of deionized water using sonication bath (5M) for 30 minutes. The silver nanoparticles stock solution was stored at 4 ^{o}C and used in antioxidant assays of ABTS, DPPH, Iron chelating, FRAP and NO radicals scavenging.

3.2.6.4 2,2'-azino-bis(3-ethylbenzothiazoline-6-sulphonic acid (ABTS)
Radical Scavenging Activity Assay

The assessment of ABTS radical scavenging activity in silver nanoparticles sample was carried out by referring to the method from Anto Cordelia, et al. (2016). The 8 mg/ml ABTS stock solution was prepared by mixing 0.04 g ABTS in 50 ml deionized water and 0.0264 g of potassium persulfate (1.32 mg/ml) ($K_2S_2O_8$) in 20 ml deionized water. The mixture of ABTS and 1.32 mg/ml $K_2S_2O_8$ was left at room temperature in dark condition for 16 hours before use. 1 M dipotassium hydrogen phosphate (K_2HPO_4) stock solution and 1 M potassium dihydrogen phosphate (KH_2PO_4) stock were prepared by dissolving 3.48 g K_2HPO_4 in 20 ml deionized water and 2.72 g KH_2PO_4 in 20 ml deionized water. Next, 80.2 ml of 0.1 M K_2HPO_4 was mixed into 19.8 ml of 0.1 M KH_2PO_4 to prepare the phosphate buffer. The prepared ABTS stock solution was diluted to optical absorbance of 0.700 $\pm$ 0.005 at 734 nm with 0.1

M potassium phosphate buffer before use. The working concentration of the sample was prepared by diluting the silver nanoparticles stock solution in deionized water. The background control of the sample was also prepared by displacing the reagent with deionized water and phosphate buffer. 1 ml of ABTS working solution was then mixed into 100 µl of sample in the dark. The mixture was left for 10 minutes. The absorbance measurement was taken at 734 nm using UV-Vis spectrophotometer (GENESYS 10). Ascorbic acid with working concentration from 0 µg/ml to 60 µg/ml was served as positive control. The ABTS scavenging ability was calculated in percentage inhibition (%).

$$\text{Percentage inhibition } (\%) = (\text{Abs}_{control} - \text{Abs}_{sample} / \text{Abs}_{control}) \times 100\%$$

Where,

Abs $_{control}$ = Absorbance measurement of negative control (without sample)

Abs $_{sample}$ = Absorbance measurement of reaction (with sample)

3.2.6.5 2,2-diphenyl-1-picrylhydrazyl (DPPH) Radical Scavenging Activity Assay

The method in assessing the DPPH radicals scavenging activity of the silver nanoparticles samples was modified from Payne, et al. (2013). DPPH reagent (0.11 mM) was prepared freshly by dissolving 0.0044 g DPPH in 100 ml of methanol. The working concentration of sample was prepared by diluting the silver nanoparticles stock solution in deionized water and a background control of the sample was prepared for each working concentration. The positive control, ascorbic acid of working concentration ranges between

0µg/ml and 30µg/ml was prepared in deionized water. Next, 1ml of 0.11 mM DPPH reagent was added into 200 µl of sample or positive control and the solution was kept in dark for 60 minutes at room temperature (20 $^\circ$C). The absorbance measurement was taken at 517 nm using UV-Vis spectrophotometer (GENESYS 10). The blank for DPPH assay was prepared by mixing 1 ml of methanol and 200 µl of deionized water. The DPPH radical scavenging activity was calculated in percentage inhibition (%).

Percentage inhibition (%) = (Abs $_{control}$ – Abs $_{sample}$ / Abs $_{control}$) X 100%

Where,

Abs $_{control}$ = Absorbance measurement of negative control (without sample)

Abs $_{sample}$ = Absorbance measurement of reaction (with sample)

3.2.6.6 Iron chelating Activity Assay

The iron chelating ability of silver nanoparticles samples was measured according to the method modified from Jindal and Mohamad, (2012). To prepare 2 mM ferrous chloride solution, 0.039 g of ferrous chloride tetrahydrate was dissolved in 100 ml deionized water. 20 ml of 5 mM ferrozine solution was then prepared freshly by dissolving 0.049 g ferrozine in 20 ml deionized water away from light source. The working concentration of sample was prepared by diluting the silver nanoparticles stock solution in deionized water and a background control of the sample was prepared for each working concentration. 30 µl of ferrous chloride solution was added into 950 µl of sample and positive control and the mixture was left in the dark for 16 hours. Then, 200 µl of 5mM ferrozine was added and the mixture was allowed

to stand at room temperature for 10 minutes. 1 ml of deionized water was added into each tube and the absorbance reading was taken at 562 nm using UV-Vis spectrophotometer (GENESYS 10). EDTA was used as the positive control with working concentration of 0 μg/ml to 20 μg/ml. The assay was carried out in triplicates and the nitric oxide scavenging activity was calculated in percentage inhibition (%).

$$\text{Percentage inhibition (\%)} = (\text{Abs}_{control} - \text{Abs}_{sample} / \text{Abs}_{control}) \text{ X } 100\%$$

Where,

Abs $_{control}$ = Absorbance measurement of negative control (without sample)

Abs $_{sample}$ = Absorbance measurement of reaction (with sample)

3.2.6.7 Ferric Reducing Antioxidant Power (FRAP)

The FRAP technique modified from Settharaksa, et al. (2014) was used to evaluate the reducing power of the silver nanoparticles. Firstly, 300 mM sodium acetate buffer was prepared. 0.93 g of sodium acetate was weighed and dissolved in deionized water and 8 ml of glacial acetic acid was added to adjust the sodium acetate buffer to pH 3.6. The mixture was then added up to a final volume of 500 ml with deionized water and the buffer was stored at 4 ^{o}C. Next, 10 mM 2,4,6-tripyridyl-s-triazine (TPTZ) was prepared by dissolving 0.039 g TPTZ in 10 ml of diluted HCl (40 mM) and the solution was mixed at 50 ^{o}C in a hot water bath. Then, 20 mM of ferric chloride hexahydrate, $FeCI_3.6H_2O$ was prepared freshly by dissolving 0.054g $FeCI_3.6H_2O$ in 10ml of deionised water. 120 ml of FRAP reagent was prepared in 10:1:1 ratio of acetate buffer, 10 mM TPTZ and 20 mM $FeCI_3.6H_2O$. The working

35

concentration of sample was prepared by diluting the silver nanoparticles stock solution in deionized water and a background control of the sample was prepared for each working concentration. EDTA was used as positive control. A series working concentration of EDTA positive control was prepared in deionized water. 2 ml of FRAP reagent was added to 200 µl of positive control and sample respectively and was left at 37 $^{\circ}$C for 5 minutes. The assay was carried out in triplicates and the absorbance measurement was taken at 593 nm using UV-Vis spectrophotometer (GENESYS 10). Ferrous sulfate heptahydrate (0 to 0.40mM) was used as standard and the reducing power of sample was expressed in mM Fe^{2+} equivalent.

3.2.6.7 Nitric Oxide (NO) Radical Scavenging Activity Assay

The nitric oxide (NO) antioxidant assay used in previous study by Bhakya, et al. (2016) was used as reference to evaluate the antioxidant activity of the silver nanoparticles. 50 ml of 5.68 mM, pH 7.4 sodium nitroprusside solution was prepared in phosphate buffer saline (PBS). Griess reagent was prepared from 1 % sulphanilamide and 0.1 % N-(1-naphthyl) ethylenediamine dihydrochloride (NEDA) by dissolving 1 g of sulphanilamide and 0.1 g of NEDA in 100 ml of 5% phosphoric acid. 200 µl of 5.68 mM sodium nitroprusside was added into 800 µl of silver nanoparticles sample and the mixture was irradiated under fluorescent light source at room temperature, 15 cm distance between the sample and light source. After 30 minutes, the mixture was removed from light source and 50 µl of Griess reagent was added. The mixture was left for 10 minutes in the dark at room temperature. The negative control was prepared by replacing sample with deionized water. A

background control of silver nanoparticles was prepared by displacing sodium nitroprusside with PBS. Ascorbic acid was used as positive control. A working concentration range of 100, 200, 300, 400 and 500 µg/ ml ascorbic acid was prepared by dilution. For the blank, a mixture of 850 µl of deionized water was added with 200 µl of PBS solution. The assay was carried out in triplicates. The absorbance measurement was taken at 546 nm using UV-Vis spectrophotometer (GENESYS 10) and the nitric oxide scavenging activity was calculated in percentage inhibition (%).

$$\text{Percentage inhibition (\%)} = (Abs_{control} - Abs_{sample} / Abs_{control}) \times 100\%$$

Where,

Abs $_{control}$ = Absorbance measurement of negative control (without sample)

Abs $_{sample}$ = Absorbance measurement of reaction (with sample)

3.2.7 Antimicrobial Activity of Silver Nanoparticles

Firstly, Gram negative *Escherichia coli* and Gram positive *Staphylococcus aureus* were selected in the evaluation of antimicrobial activity in silver nanoparticles. The stock of bacteria culture broth was prepared. 1 ml of bacteria stock in 10% glycerol was mixed into 30 ml of sterilized broth and was incubated at 37 ^{o}C for 24 hours. A working concentration of bacteria was standardized at 0.500 ± 0.02 OD600. The bacteria culture plates were prepared by inoculating bacteria culture onto the agar plates using sterilized cotton swaps. A working concentration of silver nanoparticles sample (200 µg/ml to 800 µg/ml) was prepared. 10 µl of silver nanoparticles was placed on a piece of 5 mm Whatman filter paper and the paper was transferred onto the

inoculated agar. The test was repeated by using positive control, antibiotic tetracycline at concentration of 50, 100 and 50 µg/ml. The results were repeated to obtain the triplicates data. Deionized water was served as negative control in the antimicrobial test. Aseptic techniques were performed throughout the antimicrobial test.

3.2.8 Statistical Analysis

The significant correlation between content of phenolic and flavonoid with the antioxidant activity of silver nanoparticles was assessed using correlation test in GraphPad Prism 6 Demo Version. The experimental calculated percentage inhibiton (%) in antioxidant assay and the calculated TPC(mg GAE/g) and TFC(mg QE/g) values were used as correlation coefficient data and significant level was set at $P<0.05$ (two-tailed). The significant difference for the growth inhibition of different bacteria species *Escherichia coli* (Gram negative) and *Staphylococcus aureus* (Gram positive) by silver nanoparticles and positive control was evaluated using a paired parametric t test in GraphPad Prism 6 Demo Version. The experimental calculated average zone of inhibition (mm) was used as mean comparison between the bacteria species and the $p < 0.05$ (two tailed) was set as significant level.

3.3 List of Chemicals/ Reagents

Table 3.1: Chemical reagents used and their manufacturer

Chemicals/Reagents	Manufacturer /Brand
2,2'-azino-bis(3-ethylbenzothiazoline-6-sulphonic acid)	Sigma-Aldrich
2,2-diphenyl-1-picrylhydrazyl	Sigma-Aldrich
2,4,6-tripyridyl-s-triazine (TPTZ)	EMD Millipore Corporation
Ethanol	Scharlab
Aluminium chloride hexahydrate	Sigma-Aldrich
Concentrated hydrochloric acid	QRëC^{TM}
Concentrated phosphoric acid	Systerm
Concentrated sulphuric acid	Fisher Chemical
Ethylenediaminetetraacetic acid (EDTA)	QRëC^{TM}
Ferric chloride hexahydrate	R&M Chemical
Ferrous chloride anhydrous	R&M Chemical
Ferrous sulfate heptahydrate	R&M Chemical
Ferrozine	Sigma-Alrich
Folin-Ciocalteu's Reagent	R&M Chemical
Glacial acetic acid	Synerlab
L-ascorbic acid	R&M Chemical
Methanol	RCI Labscan
N-(1-Naphthyl)ethylenediamine dihydrochloride (NEDA)	Sigma-Aldrich
Phosphoric acid (ortho)	QRëC®
Phosphate buffered saline (tablets)	TaKaRa
Potassium dihydrogen phosphate	Systerm
Potassium hydrogen phosphate	Systerm
Potassium persulphate	R&M Chemical
Silver nitrate	Bendosen
Sodium acetate	QRëC^{TM}
Sodium carbonate	Systerm
Sodium hydroxide	QRëC^{TM}
Sodium nitrite	QRëC^{TM}
Sodium nitroprusside dihydrate	Sigma-Aldrich
Sulphanilamide	R & M chemicals
Quercetin hydrate	Thermofisher Acros Organics

3.4 List of Equipments

Table 3.2: Equipments used and their brand/model

Equipment	Brand/Model
Autoclave Machine	Hirayama HVE50
Bunsen burner	CAMPINGAZ
Centrifuge Machine	Dynamica Velocity 14R
Drying Oven	Memmert
Electronic balance	Sartorious
Field Emission Scanning Electron Microscope (FESEM)	JEOL USA JSM – 7610F
Fourier Transform Infrared Spectrophotometer (FTIR)	Perkin- Elmer
Freeze dryer	ScanVac – Coolsafe ^{TM}
Grinder	Rong Tsong Precision Technology co 8两装高速打碎机 (RT-08)
Hot plate	Stuart
Incubator Shakers	INFORS HT - Ecotron
Incubation oven	Binder
Micropipette	Gilson
Projector	3M
Refrigerator	HESSTAR
Sonication bath	5M
Table lamp	CHIEF DAISY (No. H1300)
UV-Vis Spectrophotometer	Thermo Scientific (GENESYS 10)
Water bath	Sastec ^{TM} FCE20 Serials
Vortex	Vortex-Genie Scientific Industries
X-ray Diffractometer (XRD)	Siemens D500

CHAPTER 4

RESULTS

4.1 Synthesis of Silver Nanoparticles

The appearance and absorption spectrum of silver nanoparticles synthesized using 10% *Artemisia argyi* and 0.01 M silver nitrate ($AgNO_3$) solution under direct sunlight was recorded and shown in figure 4.1 and figure 4.2. The color change from yellow to dark brown (Figure 4.1) was observed within 2 minutes under direct sunlight and continued to intensify after 10 minutes of reaction which indicated the successful formation of silver nanoparticles. The absorption spectrum of centrifuged and diluted (100X) silver nanoparticles solution was measured along 300 nm to 800 nm wavelength using UV-Vis spectrophotometer. The maximum absorption of dark brown color silver nanoparticles solution was detected at 450 nm wavelength.

Figure 4.1: The reaction of 10% *Artemisia argyi* and 0.01M silver nitrate solution before and after irradiation under sunlight. The mixture changes color from yellow (left) after incubation under direct sunlight for 10 minutes into dark brown solution (right).
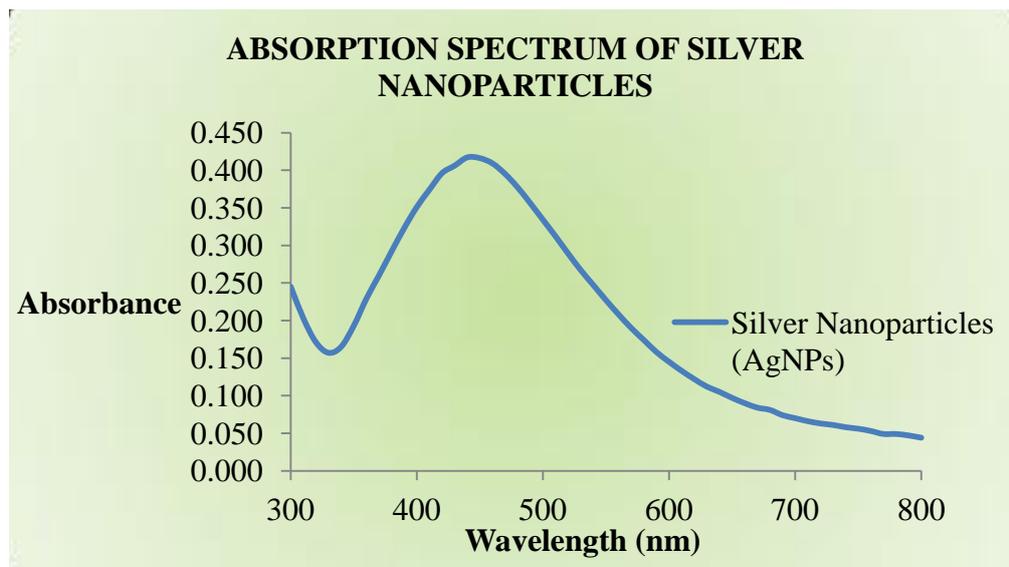
Figure 4.2: The absorption spectrum of silver nanoparticles from 300 nm wavelength to 800 nm wavelength of light.

4.2 Characterization of Silver Nanoparticles

4.2.1 UV-Vis Analysis

4.2.1.1 Appearance

The color intensity and appearance were compared among silver nanoparticles solution synthesized from 0.001 M, 0.005 M, 0.01 M and 0.05 M silver nitrate ($AgNO_3$) solution as shown in figure 4.3. The highest intensity of brown color silver nanoparticles solution formation was seen in 0.01M $AgNO_3$ solution, followed by 0.005 M $AgNO_3$, 0.05M and least in 0.001 M $AgNO_3$ solution. Visible brown large particles were formed for 0.05 M $AgNO_3$ reacted with 10% *Artemisia argyi* under projector which were failed to penetrate through the filter paper. The synthesis of silver nanoparticles from 10% *Artemisia argyi* was therefore has the optimum reaction at 0.01 M $AgNO_3$ in term of appearance and color intensity.
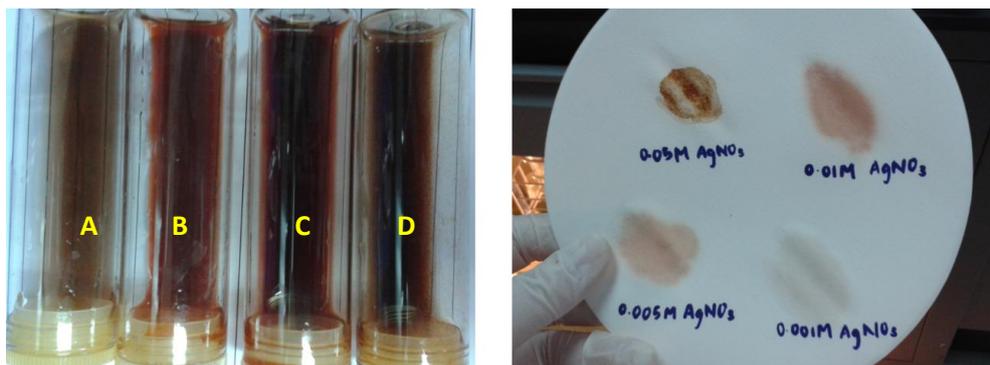
Concentration of silver nitrate concentration: (A) 0.001 M (B) 0.005M (C) 0.01 M (D) 0.05 M

Figure 4.3: The effect of silver nitrate concentration on the appearance and properties of silver nanoparticles.

4.2.2.2 Absorption Spectrum

The absorption spectrum resulted from different concentration of $AgNO_3$ with constant 10% *Artemisia argyi* extract with different concentration of silver nitrate at 0.001M, 0.005M, 0.01M and 0.05M after dilution of 20 times were measured along 300 nm to 700 nm wavelength using UV-Vis spectrophotometer as shown in figure 4.4. Based on the absorption spectrum, the absorption peaks of silver nanoparticles from 0.005 M, 0.01M and 0.05 M were visible at 450 nm, 450 nm and 430 nm respectively whereas the absorption peak was undetected in 0.001M of $AgNO_3$ within 400 nm to 500 nm wavelength which indicated the ineffective formation of silver nanoparticles using 0.01 M $AgNO_3$ for 10% *Artemisia argyi* extract. Meanwhile, the synthesized silver nanoparticles from different concentration of $AgNO_3$ possessed the highest absorption peak intensity in 0.05 M $AgNO_3$ followed by 0.01M, 0.005 M and 0.001 M of $AgNO_3$.

**ABSORPTION SPECTRUM:
EFFECT OF SILVER NITRATE**
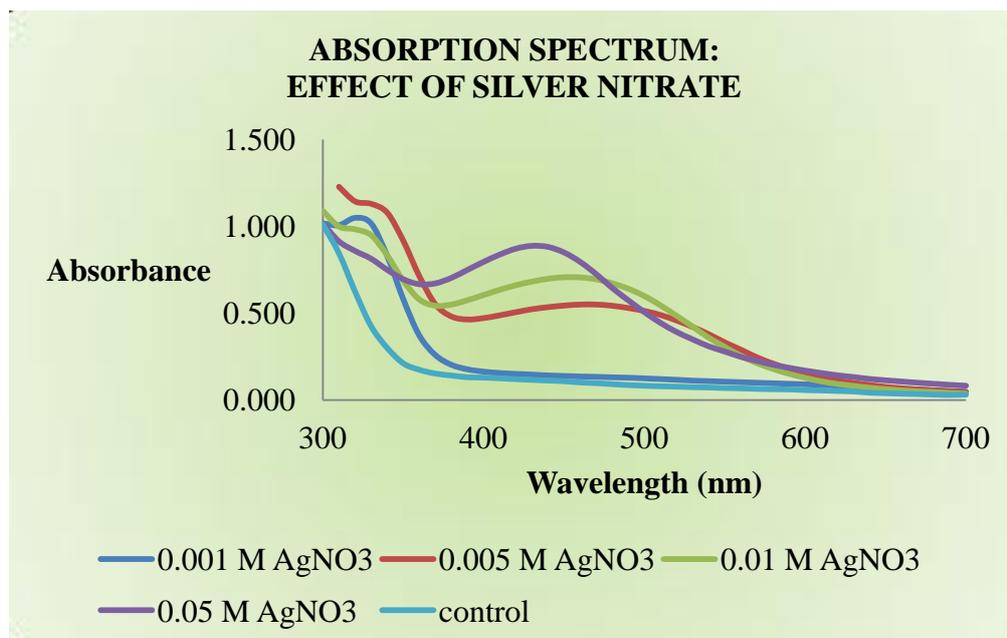
Figure 4.4: The absorption spectrum of silver nanoparticles from 300 nm wavelength to 700 nm wavelength with different concentration of silver nitrate.

4.2.3 Field Emission Scanning Electron Microscope (FESEM) Analysis

The size, shape and morphology of the freeze-dried silver nanoparticles powder produced from reaction between 10% *Artemisia argyi* extract and 0.01M $AgNO_3$ under sunlight irradiation were studied using FESEM under 100 nm as shown in figure 4.5. From the analysis of particles in FESEM, the particles were identified to range from 16 nm to 36 nm in size by ImageJ analysis and were spherical in shape.
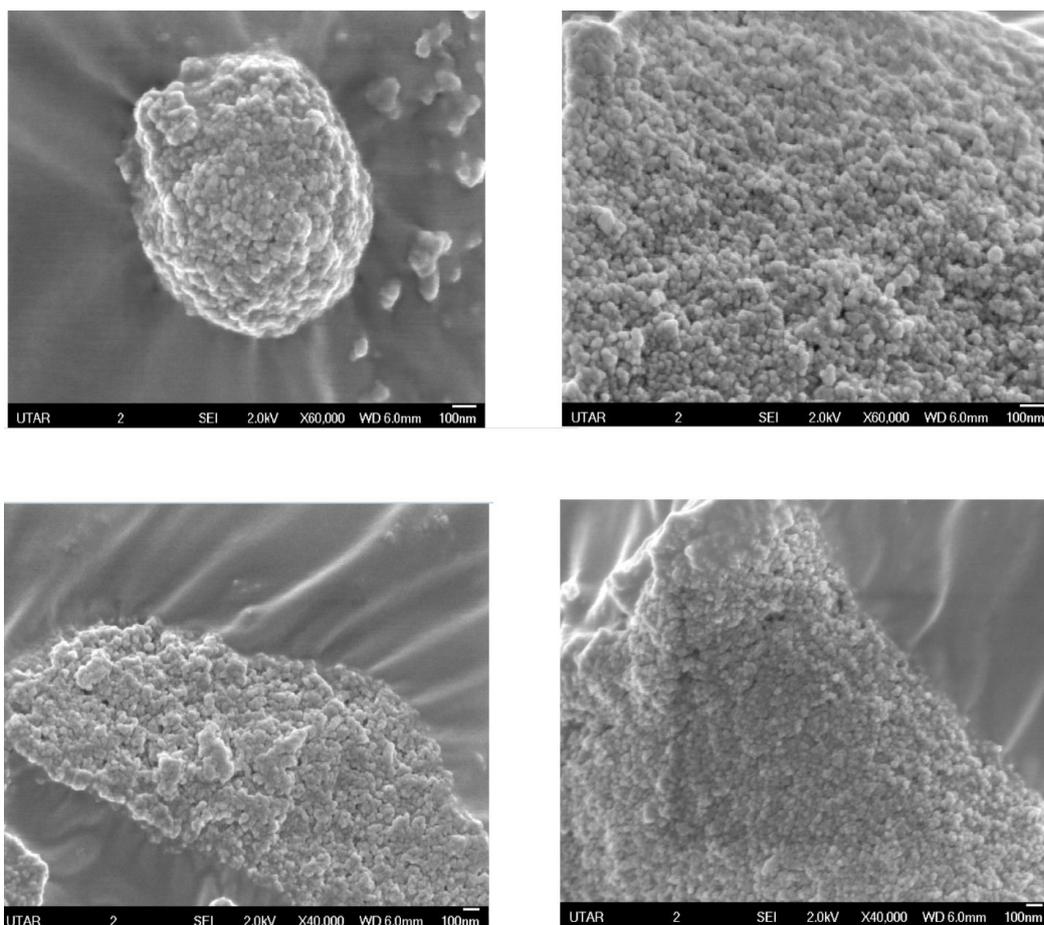
Figure 4.5: Morphology and structure of silver nanoparticles sample under FESEM at magnification of 40,000X and 60,000X.

4.2.4 Fourier Transform Infrared Spectroscopy (FTIR) Analysis

Chemical groups on the freeze-dried silver nanoparticles powder synthesized using 10% *Artemisia argyi* extract were investigated using FTIR as shown in figure 4.6. The identity of functional groups in the FTIR analysis was interpreted as shown in table 4.1. The peak at 3640 cm^{-1} was due to the amide functional group. The strongest absorption peak of the silver nanoparticles sample powder was detected at 3422 cm^{-1} and 2972 cm^{-1} represented the stretching vibration of hydroxyl group (-OH), amide (N-H) and alkanes group respectively. Sharp peaks were also detected at 2371 cm^{-1}, 2345 cm^{-1}

indicating stretch vibration of newly formed and existing C≡ N bonds from plant extract. A strong and broad peak at 1628 cm^{-1} represent the primary amines (C-N) that overlap the carbonyl stretch (C=O) and aromatic C=C stretch. Peak at1400 cm^{-1} represent the aromatic C=C stretch in the compound while 1260 cm^{-1} and 1055 cm^{-1} represent the C-N (amines) stretching vibrations. The functional groups were also detected in the plant extract (Appendix A) except for amide group at 3640 cm^{-1} and nitriles group at 2371 cm^{-1}.
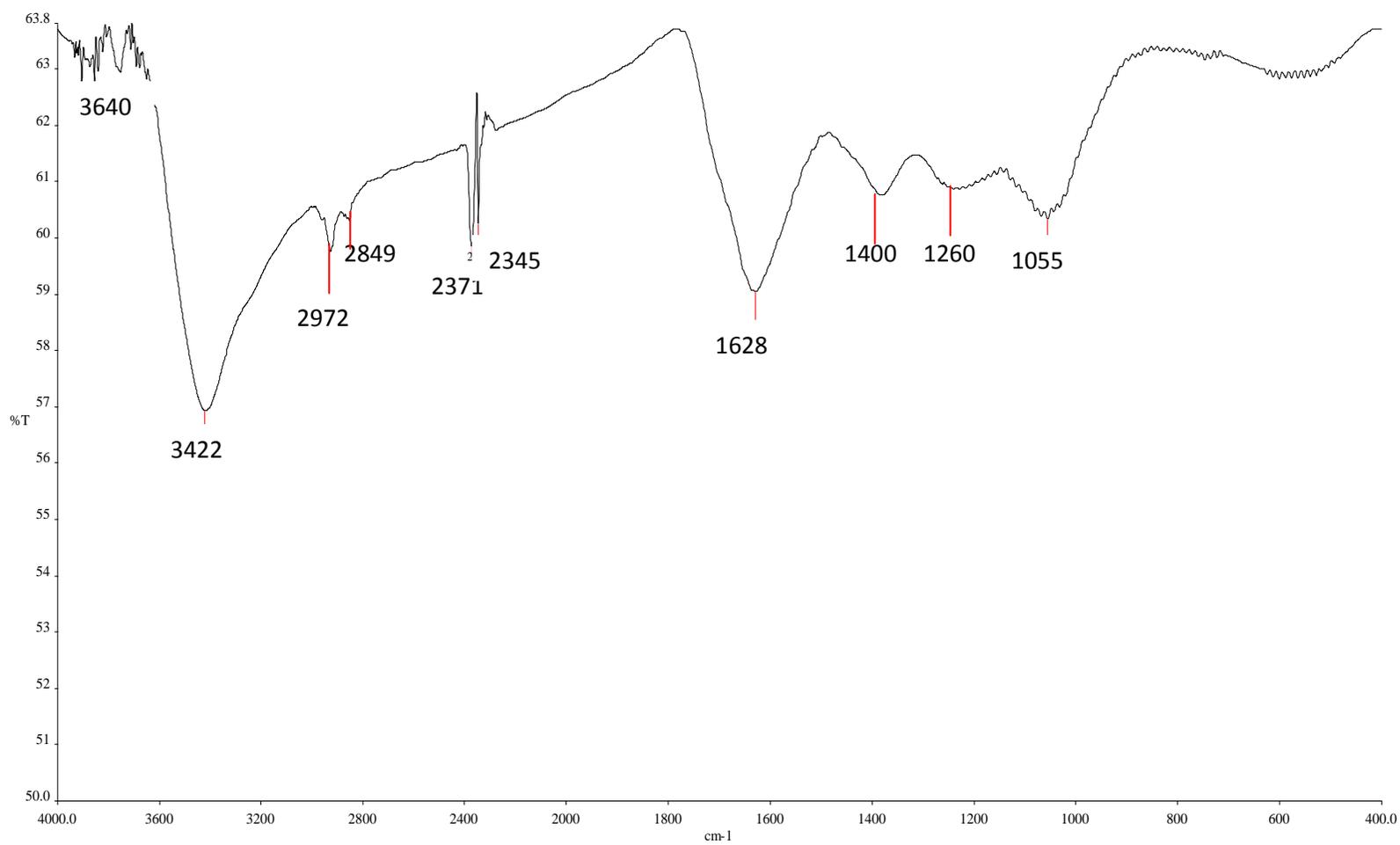
Figure 4.6: FTIR analysis of silver nanoparticles in freeze dried powder.

Table 4.1: The FTIR analysis and their interpretation on the functional groups and similarity in *Artemisia argyi* plant extract

Wavenumbers (cm^{-1})	Functional group	Compound	Detection in *Artemisia argyi*
3640	Amide (N-H)	Amide	No
3422	Hydroxyl (-OH)	Alcohol, carboxylic acids	Yes
	Amide stretch (N-H), overlapped	Secondary amide	Yes
2972	Alkane	Asymmetric alkynes	Yes
2371	Nitriles (C≡ N)	Nitriles	No
2345	Nitriles (C≡ N)	Nitriles	Yes
1628	Carbonyl stretch (C=O), overlapped	Ketones, carboxylic acids	Yes
	Carbonyl stretch (C=O), Amide (N-H), overlapped	Amide (OCNH)	Yes
	Amine (NH2)	Primary amines	Yes
	Aromatic stretch (C=C), overlapped	Aromatic ring	Yes
1400	Aromatic stretch (C=C)	Aromatic ring	Yes
1260	Amine stretch (C-N)	Aliphatic amines	Yes
1055	Amine stretch (C-N)	Aliphatic mines	Yes

2.5 X-Ray Diffraction (XRD) Analysis

The crystal structure of silver nanoparticles was studied using XRD as shown in figure 4.7 and the related values are presented in table 4.2. The pattern of the XRD peaks in the silver nanoparticles was evaluated based on the reference in JCPDS file no. 04-0783. Peaks detected at 38.77^o, 45.15^o, 64.68^o and 77.46^o were corresponding to their lattice parameters of (111), (200), (220) and (311) respectively showed the presence of silver crystals of face centered cubic structure. The average experimental lattice constant of 4.048 ± 0.018Å was compared to the theoretical value of silver of 4.085 Å. Minor impurities were also detected, marked with asterisk (*). The presence of silver chloride as secondary phase was detected at 28.38^o, 32.82^o, 46.78^o, 55.37^o, 58.18^o, and 65.46^o as referred to the JCPDS file no.85-1355. The size distribution of the silver nanoparticles was determined to be 7.63 nm, 14.38 nm, 14.44 nm and 7.56 nm at respective peaks by substituting FWHM from the peak and k of 0.9 into Scherrer's equation which gave rise to the average crystallite size of 11.00 ± 1.97 nm.
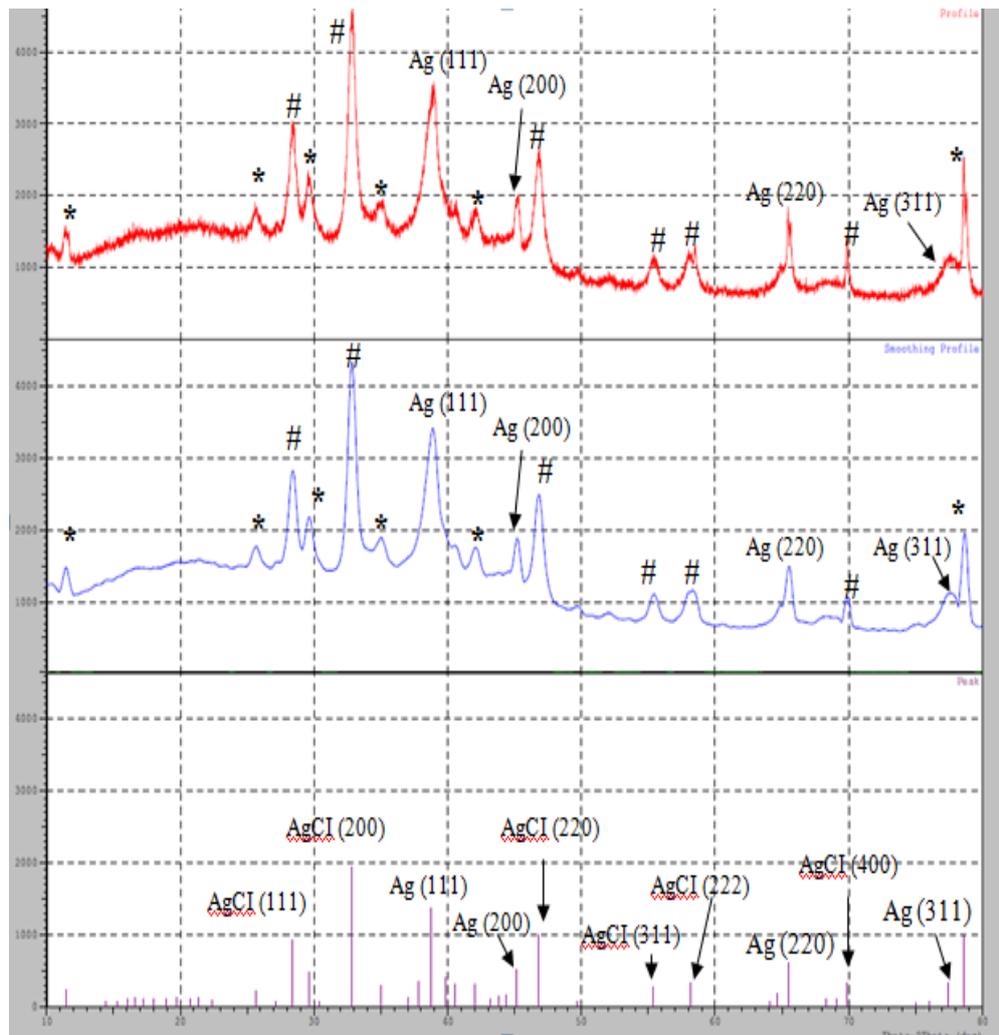
The detection of impurities were labeled as asterisk (*) and secondary phase (#) in the profile and smoothing profile. Note that the peak profile was labeled with the planes of crystallite phase, Ag and secondary phase, AgCINPs.

Figure 4.7: XRD spectra of silver nanoparticles.

Table 4.2: The experimental values of XRD analysis in silver nanoparticles sample with the calculated lattice constant, planes and size distribution

Peak No.	2Theta (degree)	d-value (A)	Intensity (Counts)	FWHM (radian)	Lattice constant (Å)	Lattice strain	hkl	Crystallite size (nm)
22	38.77	2.321	820	0.020	4.020	0.014	110	7.63
29	45.15	2.007	310	0.011	4.014	0.007	200	14.38
35	64.68	1.440	104	0.012	4.073	0.005	220	14.44
42	77.46	1.231	197	0.025	4.083	0.008	311	7.56

4.2.6 Summary of Characterization

From the UV-Vis characterization, silver nanoparticles were determined to be synthesized at optimum concentration of 0.01 M $AgNO_3$ when 10% of *Artemisia argyi* extract was used. Projector could be used as alternative source for sunlight irradiation which gave an even distribution and indirect heating to the silver nanoparticles solution. The successful formation of silver nanoparticles was determined from the dark brown color and possessed maximum absorption at 450 nm. From the microscopic analysis, the silver nanoparticles from *Artemisia argyi* were identified as spherical particles with average size of 31.97 nm. The detection of multiple functional groups such as hydroxyl group, carbonyl groups, nitriles, amines, amides and alkyne groups indicated the surface bound by phenolic groups and proteins from *Artemisia argyi*. Finally, the crystalline properties of silver nanoparticles were studied using X-Ray Diffraction in which the peaks were matched to the reference in

the JCPDS database after the purification process. The arrangement of atoms in the silver nanoparticles was determined to be in face centered cubic structure with average crystallite size distribution of 11.00 ± 1.97 nm along with coexistence of secondary phase known as silver chloride crystallites.

4.3 Total Phenolic and Total Flavonoid Content (TPC & TFC)

The content of bioactive compounds in silver nanoparticles from *Artemisia argyi* was expressed in total phenolic and total flavonoid. The content of total phenolic and total flavonoid in silver nanoparticles were studied using Folin-Ciocalteu and aluminium salts method and determined by incorporating the absorbance of silver nanoparticles measured at 725 nm and 510 nm respectively into the calibration curve of gallic acid and flavonoid as shown in figure 4.8 and figure 4.9. The absorbance readings in TPC increased linearly in accordance to the concentration of standard gave rise to regression of 0.9988 and a gradient of 5.3451 (Figure 4.8) while the points pass through the origin in the TFC, achieving regression of 0.9931 and a gradient 0.8524. From the calibration curve, the total phenolic content was determined to be 77.45 ± 0.75 mg GAE/g AgNPs while the total flavonoid content was determined to be 205.29 ± 4.11 mg GAE/g AgNPs as shown in table 4.3.
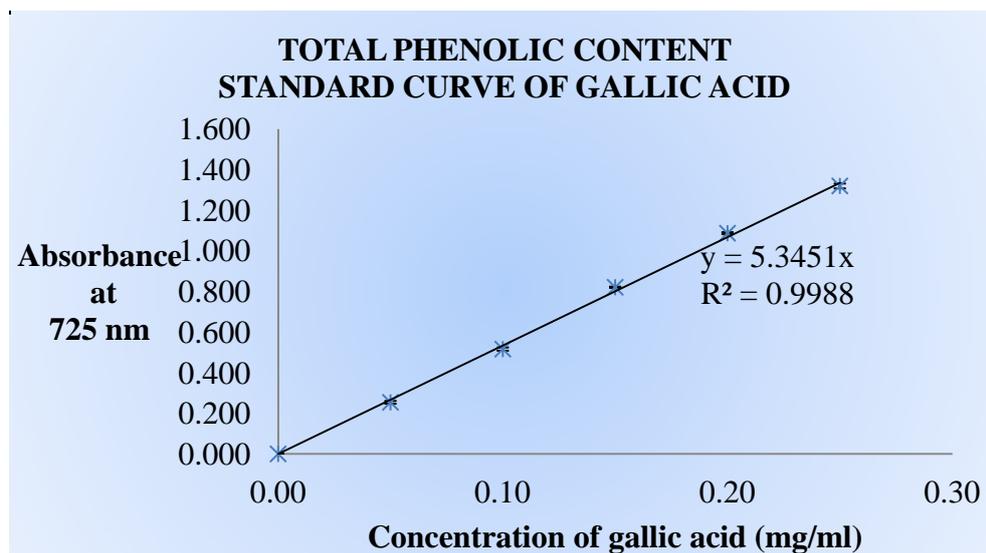
Figure 4.8: Standard curve of gallic acid in total phenolic assay.
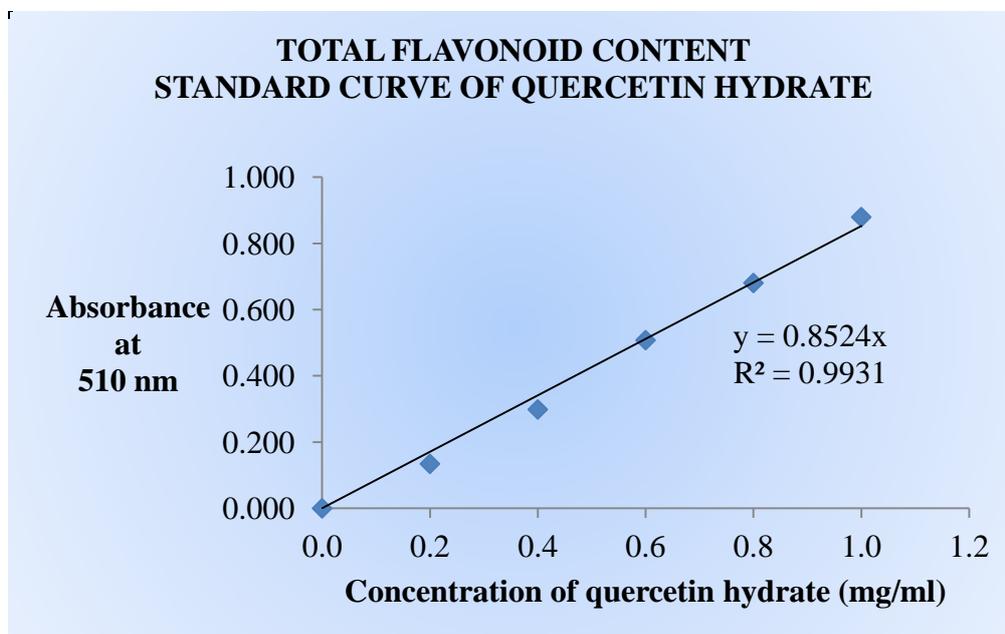
Figure 4.9: Standard curve of quercetin hydrate in total flavonoid content.

Table 4.3: The total phenolic content and total flavonoid content in mg per g dry matter of silver nanoparticles powder using *Artemisia argyi*

Bioactive compounds	Total phenolic content GAE equivalent	Total flavonoid content QE equivalent
Concentration of bioactive compounds (mg/g ± SE)	77.45 ± 0.75	205.29 ± 4.11

4.4 Antioxidant Capacity of Silver Nanoparticles

4.4.1 ABTS Radical Scavenging Activity

The ABTS scavenging activity of silver nanoparticles from 10% *Artemisia argyi* was studied in percentage inhibition (%) as shown in figure 4.10. Silver nanoparticles were shown to possess concentration dependent property in ABTS radical scavenging. The results determined the silver nanoparticles had a weaker but comparative ABTS scavenging activity than the positive control.

ABTS SCAVENGING ACTIVITY OF SILVER NANOPARTICLES

$R^2 = 0.9962$

$R^2 = 0.9991$

✳ ascorbic acid   ✳ Silver Nanoparticles
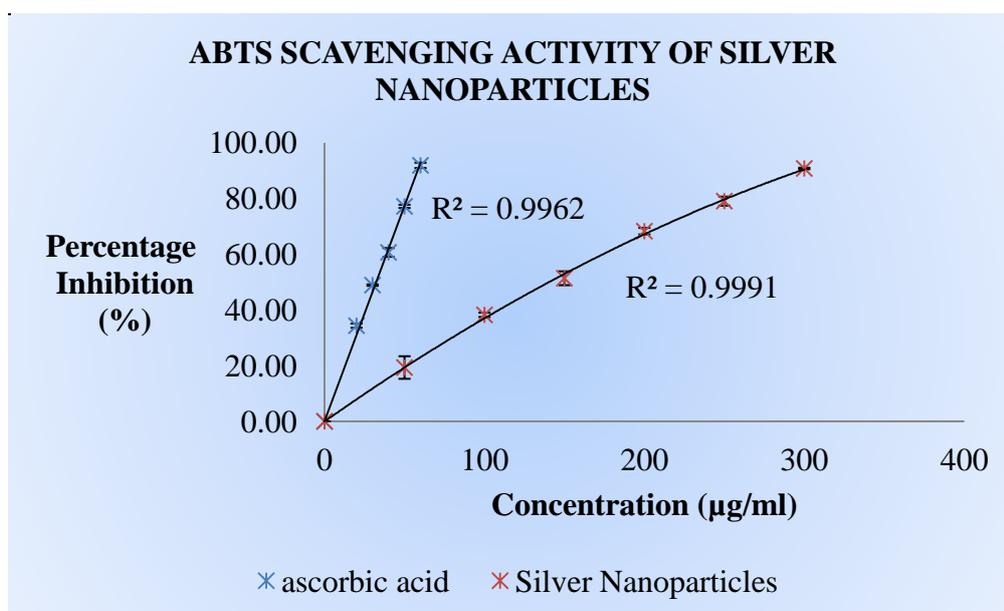
Figure 4.10: Graph of scavenging activity of silver nanoparticles on ABTS radicals in percentage inhibition (%) against concentration of solution in μg/ml.

4.4.2 DPPH Radical Scavenging Activity

The scavenging activity of silver nanoparticles from 10% *Artemisia argyi* on the synthetic DPPH radicals was expressed in percentage inhibition (%) against the concentration of sample in μg/ml as shown in figure 4.11. The DPPH scavenging activity increased as the concentration of silver nanoparticles increased in a concentration dependent manner. The silver

nanoparticles exhibited the weaker DPPH scavenging activity as compared to the positive control.

DPPH SCAVENGING ACTIVITY

$R^2 = 0.9995$

$R^2 = 0.9974$

Percentage inhibition (%)

Concentration (µg/ml)

✳ Ascorbic acid   ✳ Silver nanoparticles
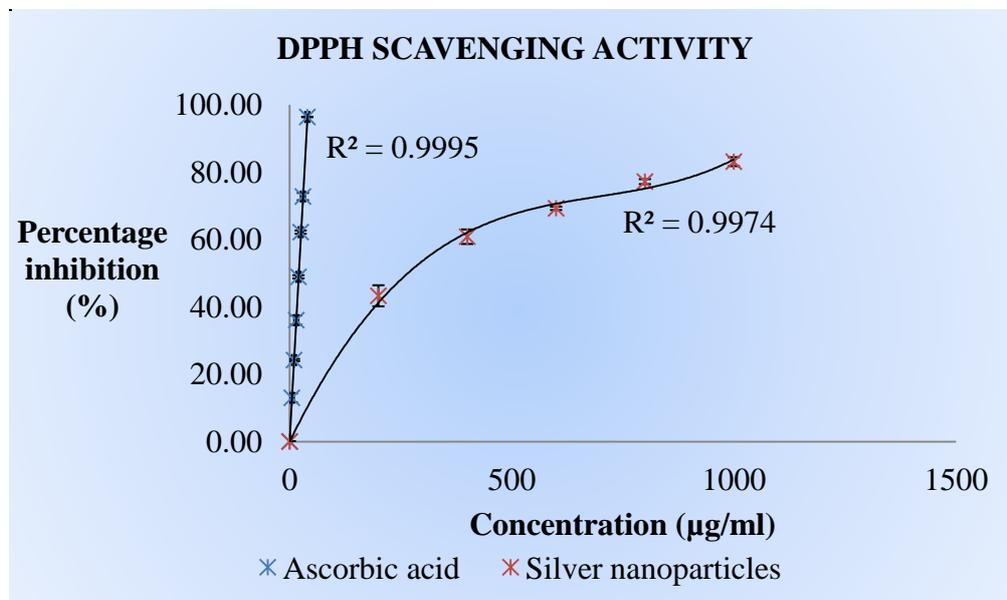
Figure 4.11: Graph of scavenging activity of silver nanoparticles on DPPH radicals in percentage inhibition (%) against concentration of solution in µg/ml.

4.4.4 Iron Chelating Activity

The iron chelating activity of silver nanoparticles from 10% *Artemisia argyi* was studied in percentage inhibition (%) as shown in figure 4.12. The iron chelating activity of silver nanoparticles was weaker and slower than that of EDTA standard but with a concentration dependent property.
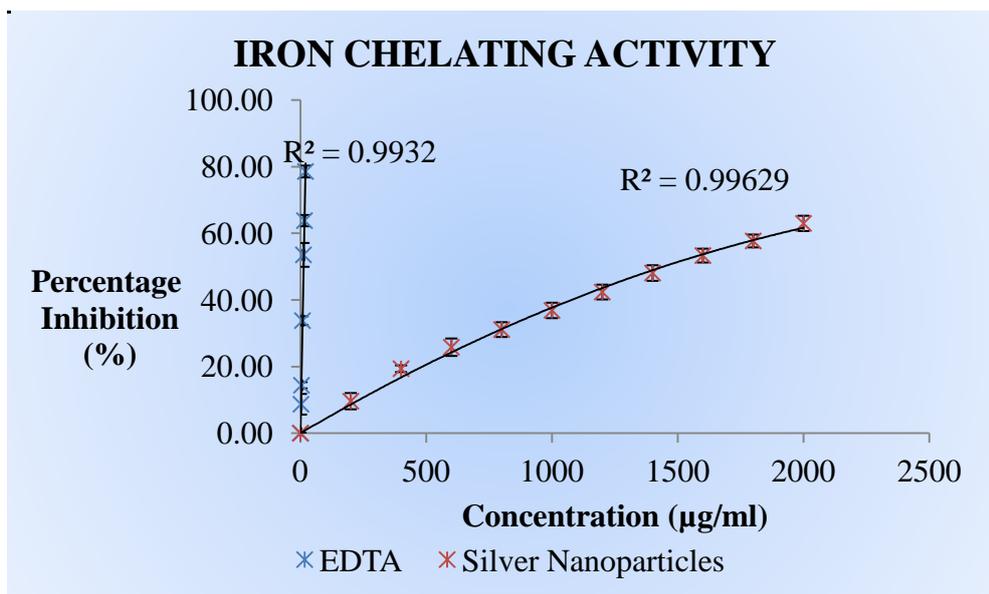
Figure 4.12: Graph of iron chelating activity in silver nanoparticles in percentage inhibition (%) against concentration of solution in µg/ml.

4.4.5 Determination of FRAP

The reducing power of silver nanoparticles from 10% *Artemisia argyi* was expressed in FRAP value as shown in figure 4.14 using standard curve from figure 4.13. In the standard curve, the points passed through the origin, achieving regression of 0.9965 and a gradient 2.5319. The reducing power of silver nanoparticles was weaker and slower than that of positive control but with a concentration dependent property.

ANTIOXIDANT ACTIVITY: FRAP STANDARD CURVE OF FESO4.7H2O
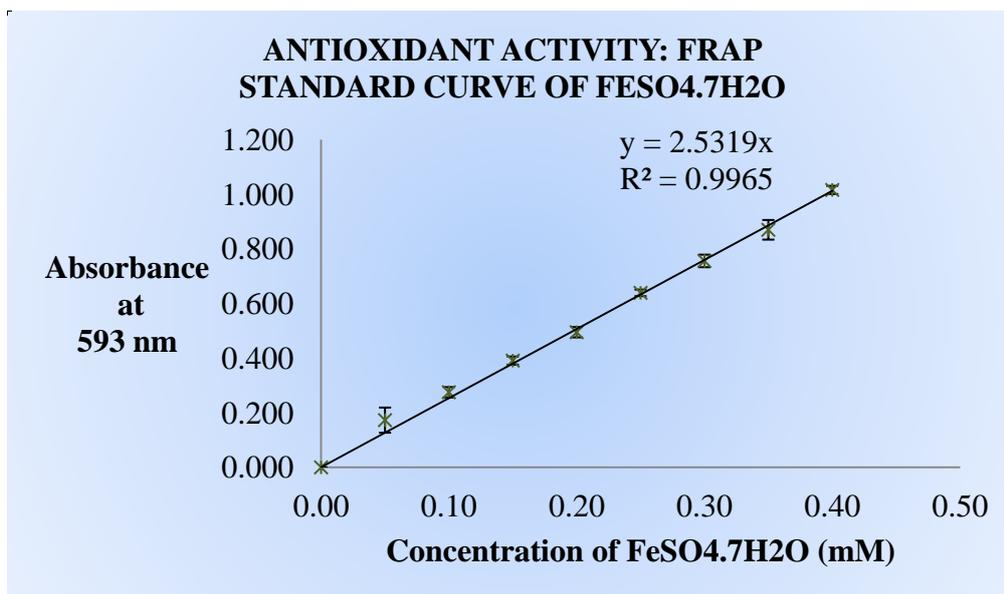
Figure 4.13: The standard curve of ferric reducing ability of plasma (FRAP) which measured at 593 nm wavelength against standard concentration of ferrous sulfate ($FeSO_4.7H_2O$) in mM.
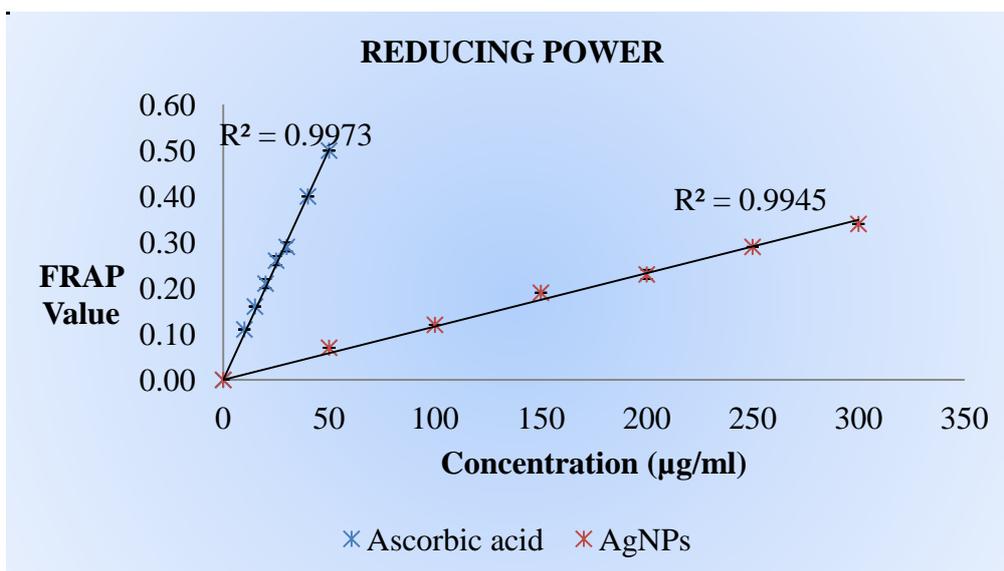
REDUCING POWER

Figure 4.14: Graph of the reducing power in silver nanoparticles in FRAP value against concentration of solution in µg/ml.

4.4.6 Nitric Oxide Scavenging Activity

The nitric oxide scavenging activity of silver nanoparticles from 10% *Artemisia argyi* was studied in percentage inhibition (%) as shown in figure 4.15. The NO scavenging activity of silver nanoparticles was concentration dependent. Silver nanoparticles were determined to scavenge the nitric oxide radicals stronger than the positive control.
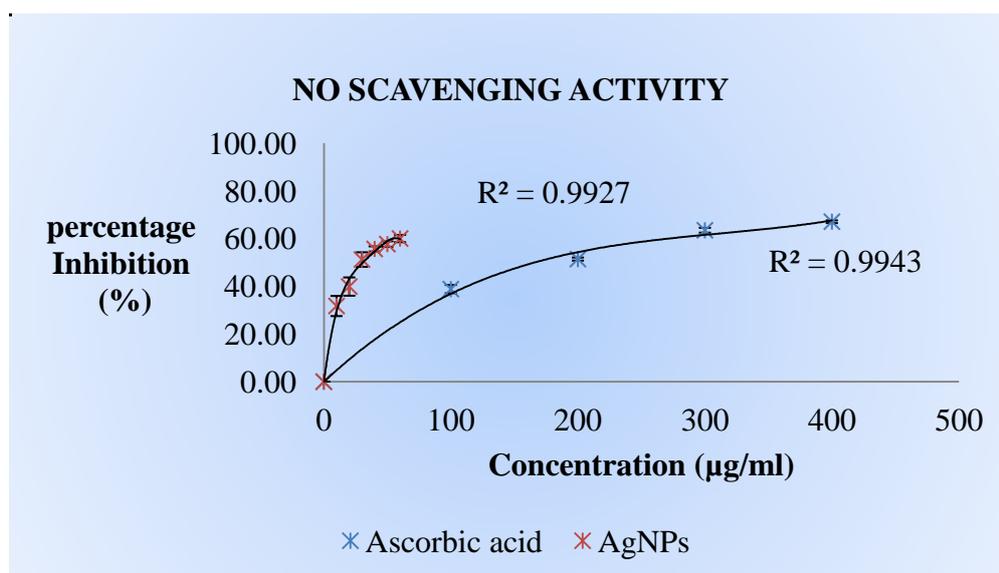
Figure 4.15: Graph of ccavenging activity of silver nanoparticles on nitric oxide (NO) radicals in percentage inhibition (%) against concentration of solution in µg/ml.

4.4.7 EC$_{50}$ of Antioxidant Capacity

The total antioxidant capacity of silver nanoparticles was evaluated in term of scavenging activity of ABTS, DPPH, iron chelating and NO radicals and reducing power. The TOAC of the control and sample silver nanoparticles was expressed in EC$_{50}$ and FRAP values as shown in table 4.4. The EC$_{50}$ was calculated using EC$_{50}$ shift in GraphPad Prism 6 Demo Version by plotting the data in a non-linear regression. Ascorbic acid was used as positive control for the assay including ABTS, DPPH, NO and FRAP except for iron chelating scavenging activity in which EDTA was used. Silver nanoparticles were calculated to possess a lower antioxidant capacity than the positive control for all the antioxidant tests except for NO scavenging activity. Silver nanoparticles from *Artemisia argyi* was an excellent scavenger for NO radicals by a successful inhibition of 50% on the radicals at 31.33 ± 0.03 µg/ml AgNPs as compared to the ascorbic acid at 172.58 ± 0.01 µg/ml. The radical scavenging activity increased in order of: NO > ABTS > DPPH > Fe^{2+} with a FRAP value of 1.22 ± 0.04 mmol Fe2+ /mg dry weight (EC$_{50}$ of AgNPs on scavenging radicals: 128.82 ± 0.02 µg/ml for ABTS; 263.03 ± 0.02 µg/ml for DPPH; 1445.44 ± 0.01 µg/ml for iron chelating; 31.33 ± 0.03 µg/ml for NO).

Table 4.4: The antioxidant capacity of silver nanoparticles from *Artemisia argyi* expressed in EC_{50} (μg/ml) and FRAP value (mmol Fe^{2+} equivalents/ mg dry weight)

Control /Sample	EC_{50} values of radical scavenging activity (μg/ml)				FRAP value*
	ABTS Scavenging	DPPH scavenging	Iron Chelating	NO Scavenging	
Ascorbic acid	29.24 ± 0.02	18.71 ± 0.02	-	172.58 ± 0.01	10.32 ± 0.17
EDTA	-	-	11.02 ± 0.01	-	-
AgNPs	128.82 ± 0.02	263.03 ± 0.02	1445.44 ± 0.01	31.33 ± 0.03	1.22 ± 0.04

* mmol Fe^{2+} equivalents/ mg dry weight

4.5 Correlation Coefficient of TPC and TFC with Antioxidant Activity

The correlation coefficient analysis of the antioxidant assay was carried out using GraphPad Prism 6 Demo Version. From the statistical analysis of antioxidant activity of silver nanoparticles as shown in table 4.5, the total phenolic and total flavonoid content of silver nanoparticles were both determined to possess significant positive correlation with the antioxidant acitivty of the silver nanopaticles synthesized from 10% *Artemisia argyi* aqueous extract in all the antioxidant assay, most significant in terms of ABTS scavenging, iron chelating and reducing power (FRAP) ($P<0.0001$ in both TPC and TFC) followed by NO scavenging (TPC: $P = 0.006$; TFC:$P = 0.0055$) and least significant in DPPH scavenging (TPC: $P = 0.0097$; TFC: $P= 0.0096$). The overall correlation coefficient between TPC/TFC and antioxidant activity of silver nanoparticles was highest in term of the reducing power, FRAP followed by ABTS, iron chelating, DPPH and least in NO scavenging activity. Besides, the TFC in silver nanoparticles was found to be correlated stronger than TPC in the ABTS, DPPH and NO scavenging while lower than TPC in the iron chelating and FRAP activities.

Table 4.5: Statistical analysis of correlation coefficient in silver nanoparticles synthesized from 10% *Artemisia argyi* extract

TOAC of Silver Nanoparticles	Total Phenolic content (TPC)		Total Flavonoid Content (TFC)	
	Correlation coefficient, r	P value	Correlation coefficient, r	P value
ABTS	0.9948	<0.0001 ****	0.9957	<0.0001 ****
DPPH	0.9184	0.0097 **	0.9189	0.0096 **
FRAP	0.9983	<0.0001 ****	0.9978	<0.0001 ****
Iron Chelating	0.9932	<0.0001 ****	0.9931	<0.0001 ****
NO	0.8985	0.006 **	0.9015	0.0055 **

P value <0.05 is set at significant ** highly significant **** excellently significant NS Not significant at 95%

4.6 Antimicrobial Activity

The antimicrobial activity of silver nanoparticles was evaluated using Gram-positive bacteria (*Staphylacoccus aureus*) and Gram-negative bacteria (*Escherichia coli*) as shown in figure 4.17. Antibiotic tetracycline with concentration of 0.05, 0.10 and 0.15 mg/ml was used as positive control to the *Staphylacoccus aureus* and *Escherichia coli* as shown in figure 4.16 and figure 4.18. An overnight incubation for 24 hours showed that increase in concentration of silver nanoparticles resulted in slight increased in zone of inhibition. Besides, the positive control was effective against Gram positive *Staphylococcus aureus* than Gram-negative *Escherichia coli.* However, the graph of antimicrobial result in figure 4.19 showed that instead of effective against Gram positive *Staphylococcus aureus,* silver nanoparticles colloid solution was more effective against Gram-negative *Escherichia coli.*
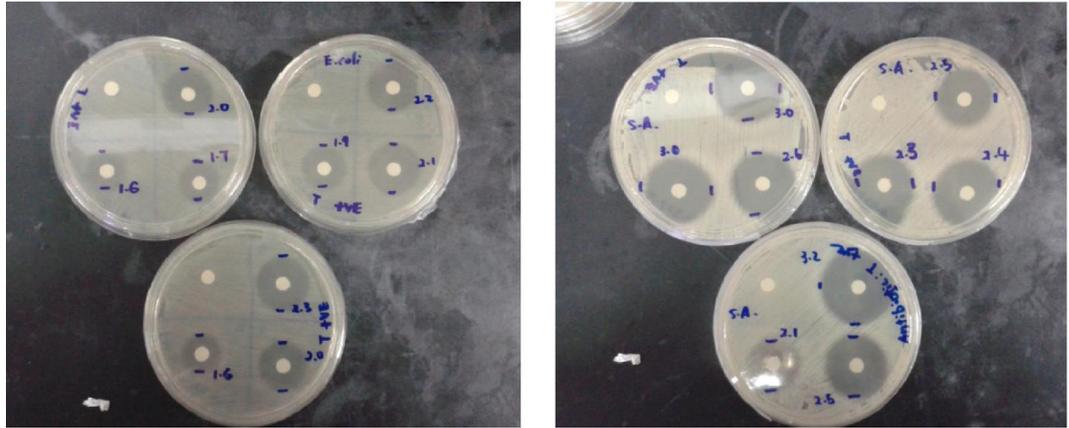
Figure 4.16: Disc diffusion test of positive control on Gram negative bacteria: *Escherichia coli* (left) and Gram positive bacteria: *Staphylococcus aureus* (right) in triplicates.
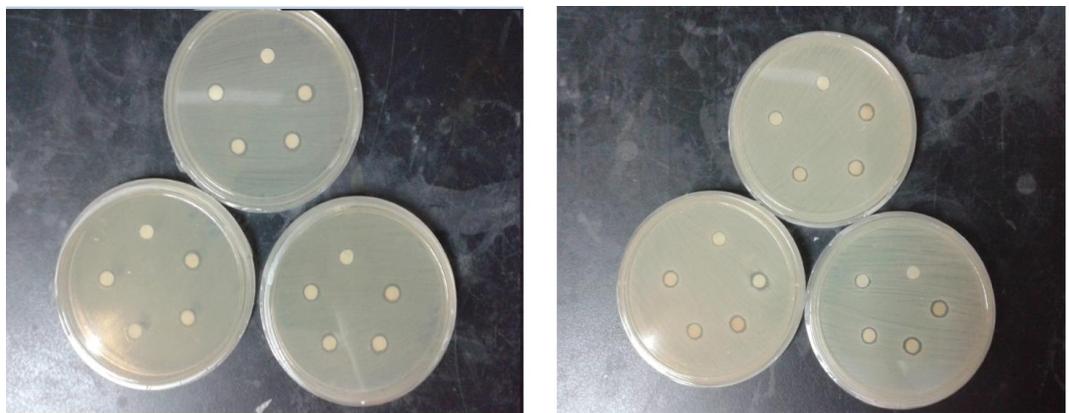
Figure 4.17: Disc diffusion test of silver nanoparticles on Gram negative bacteria: *Escherichia coli* (left) and Gram positive bacteria: *Staphylococcus aureus* (right) in triplicates.

ANTIMICROBIAL ACTIVITY POSITIVE CONTROL: TETRACYCLINE

Concentration of Tetracycline (mg/ml)	0.05	0.10	0.15
E.C.	17.0	19.3	21.7
S.A.	24.7	25.0	28.3
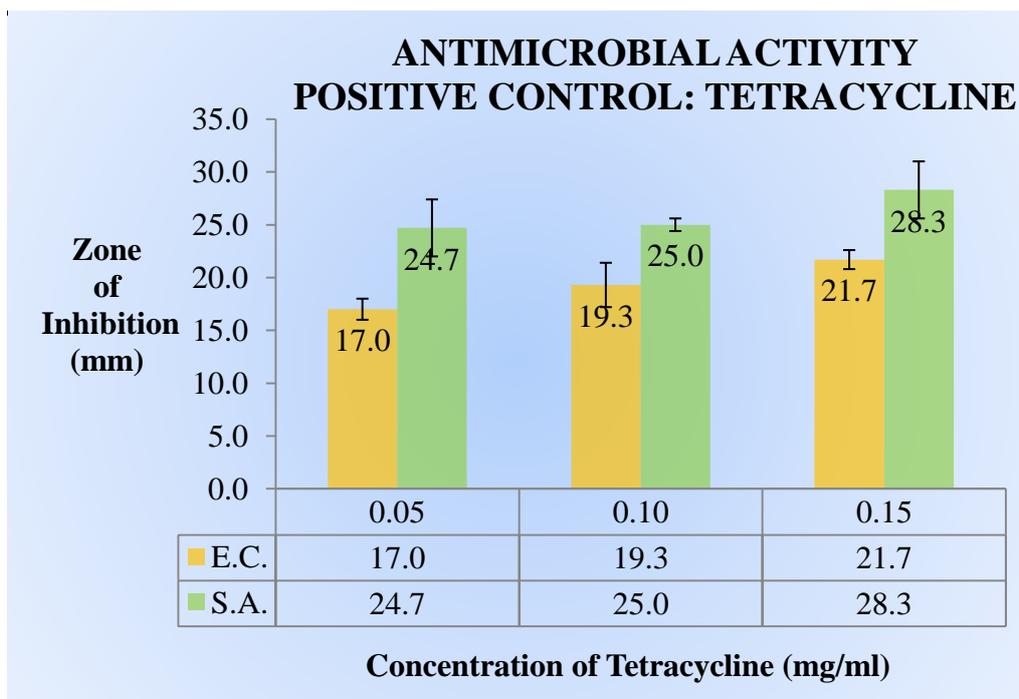
E.C. : Escherichia coli   S.A.: Staphylococcus aureus

Figure 4.18: Graph of antimicrobial activity in positive control against *Escherichia coli* and *Staphylococcus aureus* plotted in zone of inhibition (mm) against concentration of tetracycline (mg/ml).

ANTIMICROBIAL ACTIVITY OF SILVER NANOPARTICLES

Concentration of silver nanoparticles (mg/ml)	0.2	0.4	0.6	0.8
E.C.	7.6	7.9	8.2	8.7
S.A.	6.7	7.3	7.7	8.3
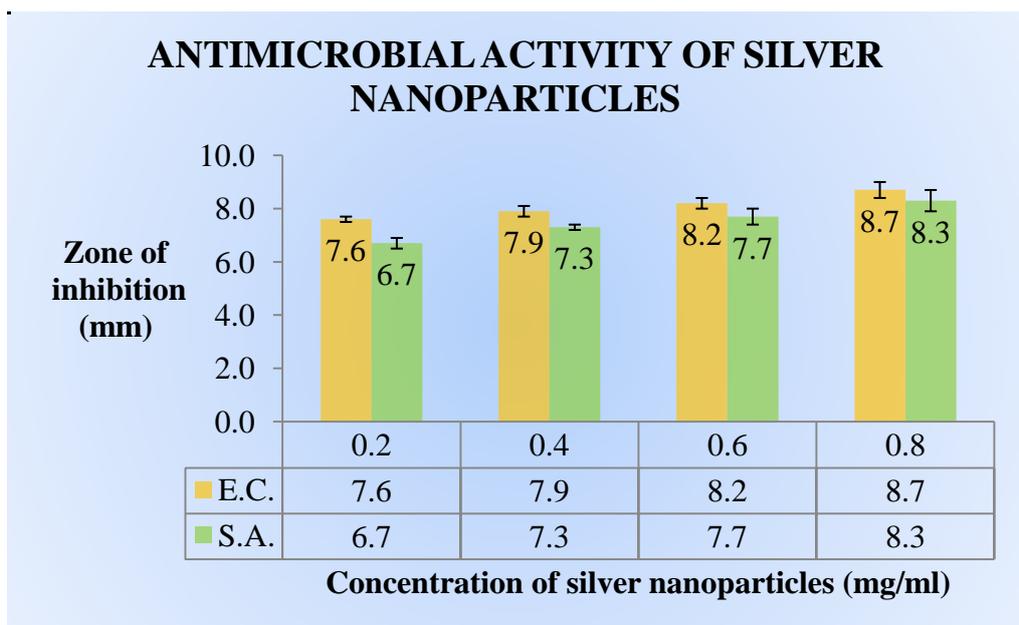
E.C. : Escherichia coli   S.A.: Staphylococcus aureus

Figure 4.19: Graph of antimicrobial activity in silver nanoparticles against *Escherichia coli* and *Staphylococcus aureus* plotted in zone of inhibition (mm) against concentration of silver nanoparticles (mg/ml).

4.7 Statistical Analysis of Antimicrobial Activity

The significant difference for the growth inhibition of different bacteria species *Escherichia coli* (Gram negative) and *Staphylococcus aureus* (Gram positive) by silver nanoparticles and positive control was evaluated using a paired parametric t test as recorded in table 4.6. The data mean was set as paired with Gaussian distribution for both positive control and sample. P < 0.05 (two tailed) was set as significant level. The result was presented in term of *Escherichia coli* against *Staphylococcus aureus*. Positive control was determined to be more effective against Gram positive bacteria as compared to Gram negative bacteria with *E.coli* versus *S.aureus* of -6.667 ± 0.578 SEM mean differences. Meanwhile, silver nanoparticles revealed the reverse of effectiveness as compared to the positive control in which the mean differences of *E.coli* versus *S.aureus* was 0.600 ± 0.108 SEM. Besides, the growth inhibition in *E.coli* by silver nanoparticles was determined to be significantly different from *S.aureus* with P value = 0.0115 which was less than 0.05 in which the differences were not due to experimental error or by random chance.

Table 4.6: Statistical analysis of mean differences in antimicrobial activity of silver nanoparticles

Differences between zone of inhibition		Paired parametric t test				
		t value	df	Means of differences ± SEM	Significant difference (P-value)	Correlation coefficient, r
E.coli vs S.aureus	TCN	11.53	2	-6.667 ± 0.578	P = 0.0074	0.9064 NS
	AgNPs	5.555	3	0.600 ± 0.108	P = 0.0115	0.9922*

P < 0.05 was set as significant level *effective significant pairing NS not significant

CHAPTER 5

DISCUSSION

5.1 Color Changes and Absorption Spectrum of Silver Nanoparticles

In this research, color changes, absorption peak and the appearance were noted in order to affirm the formation of silver nanoparticles. The silver nanoparticles are composed of nanoscale metal particles which can cause them to possess the unique property known as surface plasmon resonance (SPR) in response to the excitation of localized electrons from incident light which will cause an unusual wider scattering of light than a usual metal (Lee, et al., 2008; Baba, et al., 2014; Mahmudin, et al., 2015; Zhang, et al., 2016). In biosynthesis, this phenomena is accompanied by the reduction of silver ions into silver atoms by reducing agents from living organisms followed by the rearrangement of silver atoms into silver nanoparticles (Hussain, et al., 2011; Alagumuthu and Kirubha, 2012; Tran, Nguyen and Le, 2013). Upon the addition of plant extracts *Artemisia argyi* into silver nitrate solution, the color changed from transparent to clear yellow and into dark brown solution in respond to the formation of silver nanoparticles after irradiation under the sunlight which is the primary indicator of successful conversion of silver ions into silver nanoparticles. Meanwhile, the absorption of light within 400 nm to 500 nm with maximum absorption at 450 nm in the UV-Vis spectrum was also caused by the resonant oscillation of conduction electrons in the silver nanoparticles. The resonant of strong light absorption and scattering of light under the plasmon resonance spectra were influenced by the current shape and

size distribution of the synthesized silver nanoparticles. Similarly, the previous studies showed that the brown color formation and variation of light absorption peaks within 400 nm to 500 nm were formed due to the resonant frequency caused by the shape and size of the synthesized silver nanoparticles (Shrivastava1, et al., 2007; Hussain, et al., 2011; Verma and Mehata, 2015; Phull, et al., 2016). Together, these two features were used to affirm the successful conversion of silver nanoparticles from silver ions in accordance to their surface plasmon resonance principle.

5.2 Effect of Silver Nitrate

The UV-Vis spectrophotometry was used to study the effect of using different concentration of silver salts on the formation of silver nanoparticles. In the formation of silver nanoparticles, silver nitrate was used as primary source to provide the silver ions. As concentration of silver salts varies, the color intensity will also vary such that the increasing intensity of the brown color was spotted in the previous studies when the incubation time and concentration of silver nanoparticles increased (Ibrahim, 2015; Verma and Mehata, 2015). The similar outcome was observed in terms of the increasing intensity of brown color from the use of 0.001 M and 0.005 M to 0.01 M silver nitrate. The increasing intensity of brown color indicated the increasing of silver nanoparticles been synthesized and this was due to the increasing silver ions in the mixture.

As nanoparticles are nanoscale in size, they are not supposed to be visible to the naked eyes and should have an excellent penetration. This statement was also in agreement with the National Nanotechnology Initiative, 2000 in the nanotechnology. This explained the observation of non-observable nanoparticles by naked eyes and possession of penetration ability in the silver nanoparticles synthesized using concentration from 0.001 M to 0.01 M silver nitrate (Figure 4.3). However, the use of 0.05 M silver nitrate had showed some adverse effects in terms of clusters formation in the solution and decreasing color intensity. The formation of silver nanoparticles clusters was caused by its relatively unstable high energy surface which was not been successfully stabilized as compared to the successful protein coated silver nanoparticles, a condition that resembled the agglomeration of nanoparticles. The formation of agglomerated nanoparticles has also been observed as flocculates in previous study by Herrera, et al. (2005). The abnormal silver nanoparticles formed also caused a shift to shorter wavelength of light as analyzed from UV-Vis spectrophotometer. Theoretically, the SRP is size and shape dependent in which the decreased in size will shift the wavelength to a shorter wavelength (Mahmudin, et al., 2015; Zhang, et al., 2016). However, due to the presence of some unsuccessful coated nanoparticles, it could have caused a shrink in their size and resulted in a shift to shorter wavelength in the resonant spectra.

Although we assumed that higher concentration of silver nitrate increases the rate of silver nanoparticles formation, it should be noted that the reduction reaction would require a proper balancing between reducing agents and silver

ions. This was proven by the increasing intensity of the silver nanoparticles solution until the formation of abnormal cluster of silver nanoparticles occurred at highly concentrated silver nitrate not only in this research but similar outcomes were also obtained in previous studies which showed a drop or stunted rise in the absorption intensity of the silver nanoparticles when higher concentration of silver nitrate was been used by Ibrahim (2015), Ahmed, et al. (2015) and Khalilzadeh and Borzoo (2016). This result showed that when the source of silver is too concentrated, it can distort the balancing and proper interaction between chemicals which affects the nucleation and stabilization process to cause the formation of undesirable highly unstable clusters of silver nanoparticles that lead to the shift in resonant spectra. Therefore, the formation of silver nanoparticles can be influenced by concentration of silver salts. In this research, 0.01 M silver nitrate was determined as optimum concentration of silver salts for the formation of silver nanoparticles using 10% *Artemisia argyi* aqueous extract.

5.3 Field Emission Scanning Electron Microscope (FESEM) Analysis

Field Emission Scanning Electron Microscope (FESEM) was used in the determination of the shape and size distribution of nanoparticles (Kalainila, et al., 2014; Logeswari, Silambarasan and Abraham, 2012). Scanning electron microscope could provide a more accurate calculation in terms of nanoparticles size as it could give the direct measurement of the observed shape and size of the nanoparticles. The use of scanning electron microscope as one of the microscopic instruments that allows accurate calculation of the nanoparticles size was also mentioned by Rahman (2016) in his analysis of

gold nanoparticles. From the FESEM analysis, the silver nanoparticles was determined to be ranging from 16 nm to 32 nm with 31.97 nm average in size. The silver nanoparticles synthesized using *Artemisia argyi* by sunlight irradiation were also determined to be spherical in shape and free from agglomeration. Therefore, in terms of size, the silver nanoparticles in spherical shape were ideal to provide a large surface area to volume. On the other hand, the resonance spectra of the synthesized silver nanoparticles as mentioned in the UV-Vis spectrophotometry analysis (Figure 4.4) was caused by the resonant frequency of these spherical shaped silver nanoparticles with size ranging from 16 nm to 32 nm. Both FESEM and UV-Vis spectrophometry analysis cooperate to determine that the silver nanoparticles of spherical shape with these range of size possessed maximum absorption at 450 nm wavelength of light.

 Several factors can lead to the formation of different shapes and sizes of silver nanoparticles such as pH, temperature, light energy and concentration of chemicals in most of the cases (Mansouri and Ghader, 2009; Amin, et al., 2012; Ibrahim, 2015). In this case, the observed size and shape of these silver nanoparticles were highly related to the high reduction rate caused by the content of reducing compounds under the influence of sunlight irradiation. Sunlight irradiated the mixture in combination with photon energy and heat energy from visible light and UV was strong enough to induce and completing the photoreduction of the silver ions into silver nanoparticles within 10 minutes. The strong energy provided by sunlight was able to cause a shorter time period for the growth of silver nanoparticles therefore allowing the

nanoparticles to remain as smaller spherical shape nanoparticles. The previous studies also showed that the increase of temperature, providing higher energy had increased the rate of reduction in silver ions (Amin, et al., 2012; Ahmed, et al., 2016).

Besides, the previous studies on the chemical synthesis of silver nanoparticles by photoreduction using UV had been investigated and did not successfully produce a well distributed silver nanoparticles (Courrol, Silva and Gomes, 2007; Omrani and Taghavinia, 2011; Abdullah, Kadhim and Hilal, 2016). In contrast, the use of sunlight irradiation in the synthesis of silver nanoparticles from plant extracts was found to produce a better distribution of spherical nanoparticles (Brachmari, et al., 2014; Amaladhas, et al., 2012; Hussain, et al., 2014). An earlier study of *Artemisia marschalliana* had successfully synthesized a uniform spherical shape silver nanoparticles while others such as *Artemisia absinthium, Artemisia nilagirica* and *Artemisia capilarris* showed that most of the synthesized silver nanoparticles but not all were also in spherical shapes (Vijayakumar, et al., 2013; Ali, et al., 2016; Salehi, et al., 2016; Lim, Ahn and Park, 2016). Therefore, the factors such as concentration, nature and composition of phytochemicals compounds in *Artemisia argyi* with the help from sunlight irradiation were responsible for the formation of uniform spherical shape silver nanoparticles. These nanometer sizes of spherical silver nanoparticles formed also have a large surface area to volume and will be useful for size dependent catalytic reaction.

5.4 Fourier Transform Infrared Spectroscopy (FTIR) Analysis

Fourier Transform Infrared Spectroscopy (FTIR) was used to identify the biomolecules responsible for the synthesis of silver nanoparticles. Different biomolecules such as proteins, lipids, carbohydrate, nucleic acid, primary and secondary metabolites are composed of different functional groups as reported in previous studies (Barth, 2007; Dean, et al., 2010; Natalello, Ami and Doglia, 2012; Oliveira, et al., 2015). From FTIR analysis, the functional groups such as hydroxyl group (-OH), alkane (C-H), nitriles (-C≡ N), carbonyl group (C=O), carboxylic acids (COOH), aromatic C=C stretch, amide (N-H) and amines (NH2) were used to affirm the presence of alcoholic, carboxylic, aromatic, amides, primary and aliphatic amines compounds in the silver nanoparticles. As compared to the plant extract, silver nanoparticles showed functional groups of nearly identical except for amide and nitriles functional groups at 3640 and 2371 cm^{-1}. The similar functional groups found between silver nanoparticles and plant extract substantiated that the functional groups detected in the silver nanoparticles were attributed to the phytochemical compounds from *Artemisia argyi* crude plant aqueous extract. Phenolic compounds from plant extract usually consists of hydroxyl (-OH) and carbonyl (C=O) as the main functional groups which were also detected in the previous FTIR study of plant extracts by Oliveira, et al (2015) and Bobby, et al. (2012). The presence of alcohol groups in combination with the aromatic rings and ketones groups was therefore determined the presence of the phenolic and flavonoid compounds in the plant extract which possessed the ability to reduce metal ions of silver (Ag$^+$) into silver atoms (Ag^0). On the other hand, proteins which possessed various functional groups such as amide,

amine and carboxylic acids were involved in the stabilization of silver nanoparticles as capping agents. This was supported by the detection of amide, amine and carboxylic acids functional groups in the silver nanoparticles from the FTIR analysis. The proteins from the plant extract stabilized the nanoparticles through protein ligand binding to the metal by various weak bonds such as hydrogen, ionic bonds, hydrophobic interaction or Van Der Waals interaction (Du, et al., 2016). The detection of newly formed amide functional group also supported the formation of new protein bonds on the surface of silver nanoparticles as capping agents to further prevent the agglomeration of nanoparticles. As compared to other similar studies on silver nanoparticles, functional groups from both proteins and phenolic groups were detected as well which were claimed to be involved in the reduction and stabilization of silver nanoparticles synthesis (Ibrahim, 2015; Allafchian, et al., 2016; Jyoti, Baunthiyal and Ajeet, 2016; Salehi, et al., 2016).

On the other hand, the carbon-nitrogen bonds are polar bond, unlike alkynes, they can appear above 2200 cm-1 as a stronger peak. The previous studies on the *Artemisia marschalliana, Phlomis,* banana peel also showed the formation of nitrile functional groups in the synthesized silver nanoparticles at around 2300 - 2400 cm^{-1} (Ibrahim, 2015; Allafchian, et al., 2016; Salehi, et al., 2016). An earlier study of green synthesis of silver nanoaparticles using apple extract suggested these nitrile compounds act as reducing and capping agents (Ali, et al., 2016). Besides, a chemical synthesis using stabilizing agent Trioctyl phosphine oxide (TOPO) also showed a similar result (Alagumuthu and Kirubha, 2012). In contrast, a chemical synthesis study using similar chemical synthetic reducing agent showed that the nitrile group was absent under the

absence of stabilizing agents (Tajdidzadeh, et al., 2014). Therefore, the nitrile groups besides proteins were determined as part of stabilizing agents by contributing to the solubilization of silver nanoparticles in aqueous solvent. This can be explained by the polarity of the nitrile groups due to the electronegative N atom in which they could help in stabilizing the silver nanoparticles in the aqueous solution. On the other hand, the presence of polar nitrile groups also helped to explain the shift of light absorption to the short wavelength caused by highly concentrated silver nitrate during the formation of silver nanoparticles. The nitrile groups enabled the silver nanoparticles to acquire solubility in the solution in which the malformed silver nanoparticles were able to disaggregate upon dilution with aqueous solution into their respective size and shapes of higher resonant frequency and gave rise to the left shift in the resonant spectra as shown in Figure 4.4. Therefore, phenolic, proteins and nitrile groups are responsible for reducing, capping and stabilizing the synthesized silver nanoparticles.

5.5 Crystalline Structure of Silver Nanoparticles

The crystalline nature of silver nanoparticles was studied using X-Ray Diffraction (XRD) to understand the structure and arrangement of silver atoms. From the XRD result, the planes (111), (200), (220) and (311) reflected the face centered cubic structure of silver crystals. The average experimental lattice constant was determined to be 4.048 ± 0.018Å as compared to the theoretical value of 4.085 Å in silver. The matching of lattice parameters and lattice constant determined the face centered cubic structure in the silver nanoparticles. In the silver nanoparticles synthesized using *Artemisia argyi*,

the presence of secondary phase was also been detected. It was identified to be the silver chloride crystallites as referred to the JCPDS file No.85-1355 corresponded to the planes (111), (200), (220), (311), (222) and (400) respectively. According to Zhu, Chen and Liu (2012), the formation of silver chloride was due to the oxidation of metallic silver by hydrogen peroxide and further undergone chlorination into silver chloride nanoparticles. Hydrogen peroxide is also a compound that is naturally produced in the plants during stress condition and had been detected in a few studies (Zhou, et al., 2006; Junglee, et al., 2014; Neill, et al., 2012). Plant under same family known as *Artemisia marschalliana* by Salehi, et al. (2016) also showed a similar result as *Artemisia argyi* in the synthesis of silver nanoparticles with the existence of silver chloride nanoparticles due to the chlorine element from the plant extract. The presence of chlorine elements was also confirmed by EDAX analysis in previous studies proving similar results (Anandalakshmi, Venugobal and Ramasamy, 2015; Ibrahim, 2015; Bhakya, et al., 2016; Mahendran and Kumari, 2016). The existence of silver chloride nanoparticles were also reaffirmed by comparing the synthesized silver chloride nanoparticles to the chemical synthesis of silver chloride nanoparticles which showed a similar outcome (Dhas, et al., 2014 and Zhu, Chen and Liu, 2012). From the calculation of peak area the average crystallite size of silver nanoparticles was determined to be 11.00 ± 1.97 nm. Minor impurities were also detected which could be caused by the internal stress of amorphous organic phase from the *Artemisia argyi* plant extract as discussed in earlier studies which were explained as the crystallization of phytochemicals from plant extract.

5.6 Total Phenolic and Flavonoid Content

Phenolic and flavonoid compounds are secondary metabolites produced by plants in defense against the environmental stress condition. The phenolic and flavonoid compounds in the silver nanoparticles were determined to be 77.45 ± 0.75 GAE mg/g and 205.29 ± 4.11 QE mg/g respectively. When the content of these compounds in silver nanoparticles was compared to the previous study of local *Artemisia argyi* aqueous extract by Anto Cordelia, et al., 2016, the concentration was found to have clearly increased. First of all, the silver nitrate and plant extract was added in 9:1 proportion which indicated that there is reduction in the amount of phytochemicals in the synthesized silver nanoparticles. However, instead of showing a lower total phenolic and flavonoid content, it was found to possess a higher total phenolic and flavonoid content than the crude plant extract. Besides, silver nanoparticles in previous studies have also reported to contain a higher phenolic and flavonoid content than the plant extract (Abdel-Aziz, et al, 2014; Patra and Baek, 2016; Phull, et al., 2016). This could indicate that the antioxidant compounds expressed themselves better when adsorbed to the surface of silver nanoparticles for a more efficient complex formation between the functional groups from chemical reagents and antioxidant compounds.

5.7 Antioxidant Activity of Silver Nanoparticles

Antioxidant assays of ABTS, DPPH, iron chelating, FRAP and NO scavenging were conducted in order to study the antioxidant capacity of the green synthesized silver nanoparticles using *Artemisia argyi* as reducing agent.

In the ABTS radical scavenging activity assay, silver nanoparticles successfully reduced the $ABTS^-$ radicals in a dose dependent manner by donating the electrons from the O-H groups to reduce the $ABTS^-$ into $ABTS^{2-}$ resulting in a decreased light absorption due to the decreased in colored $ABTS^-$ radicals. Meanwhile, in the DPPH antioxidant assay, the hydrogen atoms were transferred from O-H groups on antioxidant compounds of the silver nanoparticles to the DPPH radical sites between the bulky groups and successfully stabilized them in a concentration dependent manner. In general, DPPH radicals are more stable in nature (Molyneux, 2004). However, the chemical structure of DPPH radicals should be noted since there are presences of bulky groups at the end of the DPPH radicals as described by Texeira, et al. (2013) which will cause the difficulty of hydrogen transfer from antioxidants to reach the radical site. The situation was also mentioned by Xie and Schaich, 2014 in evaluating the use of DPPH assay. This explained that the EC_{50} needed to scavenge DPPH radicals is higher as compared to NO and ABTS radicals in not only silver nanoparticles but also in most of the previous studies on the plant extracts by Mohan, et al. (2012), Anto Cordelia, et al. (2016), Chai, et al. (2014) and Wong, et al. (2014). This is primarily caused by the ineffective hydrogen atoms donating from antioxidant compounds to the radical site since DPPH radicals do not rapidly induce and accept the hydrogen atoms transferring from the antioxidant compounds. A higher amount of scavenging compounds was also needed in order to chelate the iron as some flavonoids such as naringin, pelargonidin, phloridzin and hesperitin were claimed to be ineffective in chelating iron by Van Acker, et al. (1996). Similar results on many medicinal plant extracts were reported as the *Artemisia argyi*

plant extract in terms of iron chelating activity (Mohan, et al., 2012; Chai, et al., 2014; Wong, et al., 2014). On the other hand, the ferric reducing power of silver nanoparticles was comparable to the positive control and acquired a concentration dependent reducing power. The antioxidant compounds adsorbed on the silver nanoparticles surface helped to reduce the Fe^{3+} into Fe^{2+} by donating electron to cause the increase in blue color intensity of Fe^{2+} ions. However, a remarkable nitric oxide scavenging activity in silver nanoparticles was found in which 31.33 ± 0.03 μg/ml of the silver nanoparticles could successfully scavenge 50% of the nitric oxide radicals and was more effective than ascorbic acid. This might be due to the enhanced radicals scavenging rate of the synthesized silver nanoparticles in combination with instability of nitric oxide radicals and photon energy from light illumination. The silver nanoparticles could have acted directly onto the less stable nitric oxide that have the lower bond dissociation energy (BDE) and ionization potential (IP) in energy bonding produced under light illumination before the generation of another one, causing a faster scavenging rate. The direct light illumination can play a role in the bond breaking of the antioxidant compounds by providing photon energy to excite the electron in silver nanoparticles to increase the dissociation and ionization rate of the compounds. The explanation was also in agreement with Rodriguez-Gattorno, et al. (2002) which claimed that nitric oxide can easily accept electrons from silver nanoparticles as it is relatively unstable due to the higher electronegativity on the nitric oxide radical.

5.8 Correlation Coefficient in Antioxidant Test

In the statistical analysis, the antioxidant capacity in all the assays were found to significantly possess strong positive correlations with the total phenolic and total flavonoid content in the silver nanoparticles, highest in FRAP followed by ABTS, iron chelating, DPPH and least in NO scavenging. Correlation coefficient was used to study the relationship between the total phenolic and flavonoid content with the antioxidant capacity of the silver nanoparticles. This correlation result reaffirmed that the antioxidant activity of silver nanoparticles were highly dependent on the content of phenolic and flavonoids compounds on their surfaces. The total antioxidant activity of the silver nanoparticles evaluated from the five antioxidant assays also enhanced as compared to the plant extract alone. This finding was proven by the comparison of the current result to the previous study of local *Artemisia argyi* plant extract by Anto Cordelia, et al. (2016) which showed a poorer antioxidant activity even with a higher content of antioxidant compounds than the biosynthesized silver nanoparticles along with a weak and negative correlation between the elements.

The enhancement of silver nanoparticles in antioxidant activity was first suggested by Patil and Kumbhar (2017) through the preferential adsorption of antioxidant compounds onto the surface of the silver nanoparticles therefore causing an effective scavenging ability. However, instead of preferential adsorption, the enhanced antioxidant activity could be solely caused by the enhanced expression of antioxidant functional groups through the adsorption onto the metal surface of silver nanoparticles. This was supported by FTIR

analysis which showed a similar peak pattern and intensity between the plant extract and the synthesized silver nanoparticles. This indicated that there is less likely the selective adsorption of antioxidant compounds occurred. Moreover, the silver nitrate and plant extract were added in a 9:1 ratio as mentioned which attributed that the phytochemicals available in the silver nanoparticles were in smaller amount as compared to the plant extract alone. However, the higher total phenolic and flavonoid compounds found in silver nanoparticles indicated that it was most likely affected by the way silver nanoparticles expressed the hydroxyl groups in the medium which resulted in a more efficient chemical reaction. Besides, the energy needed for ionization and dissociation of electron or hydrogen atoms of the antioxidant compounds might be overcome easily with the attachment to the metals surface of silver nanoparticles. This could be attributed to the energy exchange between metals and adsorbed molecules caused by the cloud of delocalized electrons in providing the extra strength to break the bonds for hydrogen or electron transferring. The energy transferring between metals and the molecules adsorbed on the surface was also mentioned in the chemical physical study by Egger, et al. (2015). The finding of silver nanoparticles in enhancing the antioxidant activity was in the agreement with previous studies in which a remarkable amount of antioxidant compounds was found in the green synthesized silver nanoparticles that possessed a high antioxidant capacity for various radicals (Abdel-Aziz, et al, 2014; Patra and Baek, 2016; Phull, et al., 2016; Kumar, et al., 2012; Bhakya, et al., 2016). Therefore, it would be more explainable by the silver nanoparticles acted as a medium for the adsorption of these antioxidant compounds which helped to express the functional groups on

the antioxidant compounds at higher efficiency and resulted in the more efficient hydrogen and electron transferring. This finding showed that silver nanoparticles are potent antioxidant agents when biosynthesized with plant extracts.

5.9 Antimicrobial Activity

The antimicrobial activity of silver nanoparticles was evaluated using Gram negative bacteria *Escherichia coli* and Gram positive bacteria *Staphylococcus aureus*. The exact mechanism of silver nanoparticles in antimicrobial activity is unclear and the main pathway was suggested by the releasing of silver ions and formation of free radicals that causes the inhibiton of the protein synthesis and DNA replication (Malarkodi, et al., 2013; Prabhu and Poulose, 2012). The comparison with the positive control tetracycline showed that the antimicrobial action of silver nanoparticles was different from antibiotic. The silver nanoparticles were more effective against Gram negative bacteria as compared to the positive control which was more effective against Gram positive. The diffusion of antibiotic into the bacteria cells was known to reduce due to the presence of outer cell wall on Gram negative bacteria (Delcour, 2009; Blair, et al., 2015). Nevertheless, Gram positive and Gram negative have different feature in their membrane such that thickness of peptidoglycan is higher in Gram positive and lower in Gram negative bacteria. This explained that antimicrobial activity of silver nanoparticles was found to possess inhibitory effect against both bacteria strains with higher effectiveness on Gram negative *Escherichia coli* due to the thinner peptidoglycan layer in Gram negative cell wall as compared to Gram positive bacteria. This was

similar in the antimicrobial mechanism of action in the silver ions stating that the silver ions were one of the factors responsible for the antimicrobial activity of silver nanoparticles in which the deposition of silver nanoparticles was caused by the affinity of positive charges on their surface into the negatively charged in bacterial cell wall and subsequent distortion of the membrane by the release of silver ions. However, the comparison also showed that the inhibitor activity was lower in silver nanoparticles than antibiotic. From the FTIR analysis, the protein functional groups were determined to have involved in the synthesis of silver nanoparticles. This protein coat could have decreased the effectiveness of silver nanoparticles in antimicrobial activity. The removal of protective layer of proteins on the surface of silver nanoparticles was found to increase the antimicrobial activity of the silver nanoparticles in the previous study by Jain, et al. (2015). Similar finding of higher inhibitory effect against Gram negative bacteria cells was also obtained in previous studies supporting the involvement of silver ions released from silver nanoparticles in the antimicrobial mechanism of action (Johnson and Obot, 2014; Logeswari, Silambarasan and Abraham, 2015; Allafchian, et al., 2016; Anandalakshmi, Venugobal and Ramasamy, 2016; Hussain, et al., 2016). However, further investigation should be established to understand the related factors and silver ions releasing mechanism from silver nanoparticles.

5.10   Statistical Analysis in Antimicrobial Test

Statistically, significant difference of 0.600 ± 0.108 SEM mm and a significant correlation coefficient between the bacteria strains was established between the effectiveness of silver nanoparticles and antimicrobial activities concluded that the silver nanoparticles have a higher inhibition effect against Gram negative bacteria and the correlation determined that the antimicrobial activity of silver nanoparticles was highly dependent on the diffusion rate of silver ions through the bacterial cell membrane. The silver nanoparticles are therefore effective against both bacteria strains with higher affinity towards the more pathogenic Gram negative bacteria cells depending on the diffusion rate of the released silver ions. The result also showed that the silver nanoparticles did not contribute much in the antimicrobial activity but was caused by the silver ions been released. In addition, the use of silver nanoparticles in releasing silver ions for antimicrobial purpose was claimed to be less reactive than silver ions which will be more suited for medical applications (Kim, et al., 2005).

CHAPTER 6

CONCLUSIONS

From the research, *Artemisia argyi* aqueous extract successfully synthesized the spherical shaped silver nanoparticles of size 16 nm to 32 nm through sunlight irradiation.

The phytochemical content from *Artemisia argyi* aqueous extract under the irradiation of sunlight acted as good energy source by providing efficient reduction rate for the formation of the uniform and well distributed spherical shape silver nanoparticles. Concentrated silver nitrate will also cause adverse impact on the properties of the synthesized silver nanoparticles such as occurrence of unstable agglomeration and the shift in plasmon resonant spectra.

Silver nanoparticles were proven to possess face centered cubic crystalline structure with coexistence of silver chloride crystals and phytochemicals by XRD analysis.

Besides, the FTIR analysis had supported the proteins and phenolic compounds from plant extracts in reducing silver ions and stabilizing the formation of silver nanoparticles. Newly formed nitriles groups were also determined to involve in the stabilization of silver nanoparticles in aqueous solution.

The binding of phenolic and flavonoid compounds also caused the synthesized silver nanoparticles to adapt high and concentration dependent antioxidant capacity on ABTS, DPPH, iron chelating, FRAP and most effective in NO radicals. The synthesized silver nanoparticles therefore had been proven as potent antioxidant agent when biosynthesized with plant extracts.

Lastly, the green synthesized silver nanoparticles are potent antimicrobial agent on both Gram positive and Gram negative bacteria with higher affinity towards Gram negative bacteria.

LIMITATIONS OF RESEARCH

Some limitations in this research had limited the analysis of certain features on the silver nanoparticles been synthesized using *Artemisia argyi*. First of all, unavailability of some facilities such as transmission electron microscope (TEM) and DLS had limited the finding on the detailed surface morphology and stability on the synthesized silver nanoparticles. Due to time constraint, the toxicity test, antifungal test and applications could not be carried out in this research.

FUTURE SCOPE

Antifungal test can be carried out to investigate the inhibitory effect of the green synthesized silver nanoparticles on fungus species. Characterization could have been further studied by using plant extracts synthesized using different solvents such as chloroform, acetone, hexane and ethyl acetate for examples. The phytochemicals screening on boiling method in preparing plant extracts could be further study to determine the main cause of nitric oxide scavenging in the synthesized silver nanoparticles. Anticancer test and toxicity test could be carried out to evaluate the effectiveness of silver nanoparticles on cancer disease treatment and the toxicity impact on human health.

REFERENCES

Abdel-Aziz, M.S., Shaheen, M.S., El-Nekeety, A.A. and Abdel-Wahhab, M.A., 2014. Antioxidant and antibacterial activity of silver nanoparticles biosynthesized using *Chenopodium murale* leaf extract. *Journal of Saudi Chemical Society*, 18(4), pp. 356-363.

Abdelghany, A.M., ElBatal, H.A. and ElBatal, F.H., 2015. Spectral studies of silver ions in barium borate glass and effects of gamma irradiation. *Middle East Journal of Applied Sciences*, 5(5), pp. 7-17.

Abdullah, H.I., Kadhim, K.J. and Hilal, I.H., 2016. Study the radiation time effect of synthesis silver nanoparticles by photo reduction method. *World Scientific News*, Vol. 37, pp. 220-231.

Adams, J.D., Garcia, C. and Garg, G., 2012. Mugwort (*Artemisia vulgaris, Artemisia douglasiana, Artemisia argyi*) in the treatment of menopause, premenstrual syndrome, dysmerrhea and attention deficit hyperactive disorder. *Chinese Medicine*, Vol. 3, pp. 116-123.

Adjimani, J.P. and Asare, P., 2015. Antioxidant and free radical scavenging activity of iron chelators. *Toxicology Reports*, Vol. 2, pp. 721-728.

Ahmed, S., Ahmad, M. and Swami, B.L. and Ikram, S., 2016. A review on plants extract mediated synthesis of silver nanoparticles for antimicrobial applications: A green expertise. *Journal of Advanced Research*, 7(1), pp. 17-28.

Ahmed, S., Saifullah, Ahmad, M., Swami, B.L. and Ikram, S., 2015. Green synthesis of silver nanoparticles using *Azadirachta indica* aqueous leaf extract. *Journal of Radiation Research and Applied Sciences*, 9(1), pp.1-7.

Alagumuthu, G. and Kirubha, R., 2012. Synthesis and characterisation of silver nanoparticles in different medium. *Open journal of Synthesis Theory and Application*, Vol. 1, pp. 13-17.

Alexander, J.W., 2009. History of the medical use of silver. *Surgical Infections*, 10(3), pp. 289-292.

Alfadda, A.A. and Sallam, R.M., 2012. Reactive oxygen species in health and disease. *Journal of Biomedicine and Biotechnology*. [online] Available at: < https://www.hindawi.com/journals/bmri/2012/936486/> [Accessed 2 January 2017].

Ali, M., Kim, B., Belfield, K.D., Norman, D., Brennan, M. and Ali, G.S., 2016. Green synthesis and characterization of silver nanoparticles using *Artemisia absinthium* aqueous extract — A comprehensive study. *Materials Science and Engineering C*, 58(1), pp. 359-365.

Ali, Z.A., Yahya, R., Sekaran, S.D. and Puteh, R., 2016. Green synthesis of silver nanoparticles using apple extract and its antibacterial properties. *Advances in Materials Science and Engineering*. [online] Available at: <http://dx.doi.org/10.1155/2016/4102196> [Accessed 2 March 2017].

Allafchian, A.R., Mirahmadi-Zare, S.Z., Jalali, S.A.H., Hashemi, S.S. and Vahabi., 2016. Green synthesis of silver nanoparticles using *phlomis* leaf extract and investigation of their antibacterial activity. *Journal of Nanostructure in Chemistry*, 6(2), pp. 129-135.

Amadou, I., Le, G.W. and Shi, Y.H., 2012. Effect of boiling on the cytotoxic and antioxidant properties of aqueous fruit extract of desert date, *Balanites aegyptiaca*(L) Delile. *Tropical Journal of Pharmaceutical Research,* 11(3), pp. 437-444.

Amaladhas, T.P., Sivagami, S., Devi, T.A., Ananthi, N. and Velammal, S.P., 2012. Biogenic synthesis of silver nanoparticles by leaf extract of *Cassia angustifolia*. *Advances in Natural Sciences: Nanoscience and Nanotechnology*, Vol. 3, pp.1- 7.

Amin, M., Anwar, F., Ramzan, M., Awais Iqbal, M., Rashid, U., 2012. Green synthesis of silver nanoparticles through reduction with *Solanum xanthocarpum* L. berry extract: characterization, antimicrobial and urease inhibitory activities against *Helicobacter pylori*. *International Journal of Molecular Science*, Vol. 13, pp. 9923-9941.

Anandalakshmi, K., Venugobal, J. and Ramasamy, V., 2016. Characterization of silver nanoparticles by green synthesis method using *Pedalium murex* leaf extract and their antibacterial activity. *Applied Nanoscience*, 6(3), pp. 399-408.

Anto Cordelia, T.A.D., Ti, W.M., Hnin, P.A. and Sam, J.H., 2016. Preliminary screening of *Artemisia argyi* for antioxidant potentials. *International Journal of Pharmacognosy and Phytochemical Research*, 8(2), pp. 347-355.

Araújo, E.A., Andrade, N.J., da Silva, L.H., Bernardes, P.C., de C. Teixeira, A.V., de Sá, J.P., Fialho,J.F.J., Fernandes, P.E., 2012. Antimicrobial effects of silver nanoparticles against bacterial cells adhered to stainless steel surfaces. *Journal of Food Protection*, 75(4), pp. 701-705.

Azlim Almey, A.A., Ahmed Jalal Khan, C., Syed Zahir, I., Mustapha Suleiman, K., Aisyah, M.R. and Kamarul Rahim, K., 2010. Total phenolic content and primary antioxidant activity of methanolic and ethanolic extracts of aromatic plants' leaves. *International Food Research Journal*, Vol. 17, pp. 1077-1084.

Baba, A., Imazu, K., Yoshida, A., Tanaka, D. and Tamada, K., Surface plasmon resonance properties of silver nanoparticles 2D sheets on metal gratings. *Advanced Functional Materials.* [online] Available at: <https://springerplus.springeropen.com/articles/10.1186/2193-1801-3-284> [Accessed 26 March 2017].

Barth, A., Review: Infrared spectroscopy of proteins. *Biochimica et Biophysica Acta (BBA) – Bioenergetics*, 1767(9), pp. 1073-1101.

Bendary, E., Francis, R.R., Ali, H.M.G., Sarwat, M.I. and El Hady, S., 2013. Antioxidant and structure–activity relationships (SARs) of some phenolic and anilines compounds. *Annals of Agricultural Sciences*, 58(2), pp. 173-181.

Bhakya, S., Muthukrishnan, S., Sukumaran, M. and Muthukumar, M., 2016. Biogenic synthesis of silver nanoparticles and their antioxidant and antibacterial activity. *Applied Nanoscience*, 6(5), pp. 755-766.

Blair, J.M., Webber, M.A., Baylay, A.J., Ogbolu, D.O. and Piddock, L.J., 2015. Molecular mechanisms of antibiotic resistance. *Nature Reviews Microbiology*, 13(1), pp. 42–51.

Bobby, M.D.N., Wesely, E.G. and Johnson, M., 2012. FT-IR studies on the leaves of *Albizia Lebbeck* Benth. *International Journal of Pharmacy and Pharmaceutical Sciences*, 4(3), pp. 293-296.

Boora, F., Chirisa, E. and Mukanganyama, S., 2014. Evaluation of nitrite radical scavenging properties of selected Zimbabwean plant extracts and their phytoconstituents. *Journal of Food Processing*, [online] Available at: <http://dx.doi.org/10.1155/2014/918018> [Accessed 6 September 2015].

Brahmachari, G., Sarkar, S., Ghosh, R., Barman, S., Mandal, N.C., Jash, S.K., Banerjee, B. and Roy, R., 2014. Sunlight-induced rapid and efficient biogenic synthesis of silver nanoparticles using aqueous leaf extract of *Ocimum sanctum* Linn. with enhanced antibacterial activity. *Organic and Medical Chemistry Letters*, 4(1), pp.1- 18.

Bruce, H., 2012. *Moxa Use in Pregnancy.* [e-book] Australia: Creating Living Energy Pty Ltd. Available at: < wwww.easybabies.co.au> [Accessed 10 February 2017].

Cason, J.S., Jackson, D.M., Lowbury, E.J. and Ricketts, C.R., 1966. Antiseptic and aseptic prophylaxis for burns: use of silver nitrate and of isolaters. *British Medical Journal*, 2(5525), pp. 1288-1294.

Chai, T.T., Mohan, M., Ong, H.C. and Wong, F.C., 2014. Antioxidant, iron-chelating and anti-glucosidase activities of *Typha domingensis* Pers (Typhaceae). *Tropical Journal of Pharmaceutical Research January*, 13 (1), pp. 67-72.

Chang, Y., Lu,Y. and Chou, K., 2011. Diameter control of silver nanowires by chloride ions and its application as transparent conductive coating. *Chemistry Letters*, Vol. 40, pp. 1352–1353.

Chen, H., Pu, J.S., Liu, D., Yu, W.S., Shao, Y.Y., Yang, G.W., Xiang, Z.H. and He, N.J.,2016. Anti-Inflammatory and Antinociceptive Properties of Flavonoids from the Fruits of Black Mulberry (*Morus nigra* L.). *PLOS ONE*. [online] Available at: <http://journals.plos.org/plosone/article?id=10.1371/journal.pone.0153080> [Accessed 2 March 2017].

Chu, W.B., Shi, B.L., Yan, S.M., Zhang, P.F., Zhao, F., Sun, D.S., Zhao, Q.L. and Zhang, J., 2015. Effect of *Artemisia argyi* extract on immunative and antioxidative function in broilers. *Chinese Journal of Animal Science*, 51(19), pp. 67-70.

Chopra, I., 2007. The increasing use of silver- based products as antimicrobial agents: a useful development or a cause for conceal?. *Journal of Antimicrobial Chemotherapy*, 59(4), pp.587-590.

Courrol, L.C., Silva, F.R.O. and Gomes,L., 2007. A simple method to synthesize silver nanoparticles by photo-reduction. *Colloids and Surfaces A: Physicochemical and Enginerring Aspects*, Vol. 305, pp. 54-57.

Culiţă, S. and Adrian, O., 2011. New records in the alien flora of Romania (*Artemisia argyi*, *A. lavandulaefolia*) and Europe (*A. lancea*). *Turkish Journal of Botany*, Vol. 35, pp. 717-728.

Dean, A.P., Sigee, D.C., Estrada, B. and Pittman, J.K., 2010. Using FTIR spectroscopy for rapid determination of lipid accumulation in response to nitrogen limitation in freshwater microalgae. *Bioresource Technology*, Vol. 101, pp. 4499-4507.

Delcour, A.H., 2009. Outer Membrane Permeability and Antibiotic Resistance. *Biochimica et biophysica acta*, 1794(5), pp. 808-816.

Dhas, T.S. Kumar, V.G., Karthick, V., Angel, K.J. and Govindaraju, K., 2014. Facile synthesis of silver chloride nanoparticles using marine alga and its antibacterial efficacy. *Spectrochimica Acta Part A: Molecular and Biomolecular Spectroscopy*, 120 (24), pp. 416 -420.

Drake, P.L. and Hazelwood, K.J., 2005. Exposure-related health effects of silver and silver compounds: A Review. *Annals of Occupational Hygiene*, 49(7), pp. 575-585.

Dröge, W., 2002. Free radicals in the physiological control of cell function. *Physiological Reviews,* 82(1), pp. 47-95.

Du, X., Xia, Y.L., Ai, S.M., Liang, J., Sang, P., Ji, X.L. and Liu, S.Q., 2016. Insights into protein–ligand interactions: mechanisms, models, and methods. *International Journal of Molecular Sciences*, 17(2), pp.144.

Egger, D.A., Liu, Z.F., Neaton, J.B. and Kronik, L., 2015. Reliable energy level alignment at physisorbed molecule–metal interfaces from density functional theory. *Nano Letters*, 15(4), pp. 2448 -2455.

EI-Brolossy, T.A., Abdallah, T., Mohamed, M.B., Abdallah, S., Easawi, K., Negm, S. and Talaat, H., 2008. Shape and size dependence of the surface plasmon resonance of gold nanoparticles studied by Photoacoustic technique. *The European Physical Journal Special Topics*, 153(1), pp. 361-364.

Feng, Z.V., Gunsolus, I.L., Qiu, T.A., Hurley, K.R., Nyberg, L.H., Frew, H., Johnson, K.P., Vartanian, A.M., Jacob, L.M., Lohse, S.E., Torelli, M.D., Hamers, R.J., Murphy, C.J. and Haynes, C.L., 2015. Impacts of gold nanoparticle charge and ligand type on surface binding and toxicity to Gram-negative and Gram-positive bacteria. *Chemical Science*, 6(9), pp. 5186-5196.

Fu, P.P., Xia, Q.S., Hwang, H.M., Ray, P.C. and Yu, H.T., 2014. Mechanisms of nanotoxicity: Generation of reactive oxygen species. *Journal of Food and Drug Analysis*, 22(1), pp. 64-75.

Ge, L.P., Li, Q.T., Wang, M., Ouyang, J., Li, X.J. and Xing, M.M.Q., 2014. Nanosilver particles in medical applications: synthesis, performance, and toxicity. *International Journal of Nanomedicine*, 9(1), pp. 2399-2407.

Ghasemzadeh, A. and Ghasemzadeh, N., 2011. Flavonoids and phenolic acids: role and biochemical activity in plants and human. *Journal of Medicinal Plants Research*, 5(31), pp. 6697-6703.

Giridharan, T., Masi, C., Sindhu, S. and Arumugam, P., 2014. Studies on green synthesis, characterization and anti-proliferative potential of silver nano particles using *Dodonaea viscosa* and *Capparis decidua*. *Biosciences Biotechnology Research Asia*, 11(2), pp. 665-673.

Giri, K.R., Bibek, G.C., Kharel, D., and Subba, B., 2014. Screening of phytochemicals, antioxidant and silver nanoparticles biosynthesizing capacities of some medicinal plants of Nepal. *Journal of Plant Sciences*, 2(1), pp. 77-81.

Godlewska, K., Michalak, I., Tuhy, L. and Chojnacka, K., 2016. Plant growth biostimulants based on different methods of seaweed extraction with water. *BioMed Research International*. [online] Available at: <https://www.hindawi.com/journals/bmri/2016/5973760/> [Accessed 20 March 2017].

Gottenbos, B., Grijpma,D.W., Henry,C.V.D.M., Feijen, J. and Busscher, H.J., 2001. Antimicrobial effects of positively charged surfaces on adhering Gram-

positive and Gram-negative bacteria. *Journal of Antimicrobial Chemotherapy*,48 (1), pp. 7-13.

Greenwood, N.N. and Earnshaw, A., 1997. *Chemistry of the Elements.* 2nd edition. [e-Book] Burlington: Elsevier Butterworth-Heinemann. Available at: Google Books <books.google.com > [Accessed 25 March 2017].

Gudikandula, K. and Maringanti, S.C., 2016. Synthesis of silver nanoparticles by chemical and biological methods and their antimicrobial properties. *Journal of Experimental Nanoscience*, 11(9), pp. 1745-8099.

Gupta, V.K. and Sharma, S.K., 2006. Plants as natural antioxidants. *Natural Product Radiance*, 5(4), pp. 326-334.

Guzmán, M.G., Dille, J., Godet, S., 2008. Synthesis of silver nanoparticles by chemical reduction method and their antibacterial activity. *International Journal of Chemical, Molecular, Nuclear, Materials and Metallurgical Engineering*, 2(7), pp. 91-98.

Hazra, B., Biswas, S. and Mandal, N., 2008. Antioxidant and free radical scavenging activity of *Spondias pinnata*. *BMC Complementary and Alternative Medicine*. [online] Available at: <http://www.biomedcentral.com/1472-6882/8/63> [Accessed 4 February 2017].

Herrera, A.P., Resto, O., Briano, J.G. and Rinaldi, C., 2005. Synthesis and agglomeration of gold nanoparticles in reverse micelles. *Nanotechnology*, 16(7), pp. 618-625.

Hsueh, Y.H., Lin, K.S., Ke, W.J., Hsieh, C.T., Chiang, C.L., Tzou, D.Y. and Liu, S.T., 2015. The antimicrobial properties of silver nanopaticles in *Bacillus subtilis* are mediated by released Ag+ ions. *PLoS ONE.* [online] Available at: <https://www.ncbi.nlm.nih.gov/pmc/articles/PMC4682921/> [Accessed 23 February 2017].

Huang, D., Ou, B. and Prior, R.L. 2005.The chemistry behind antioxidant capacity assays. *Journal of Agricultural and Food Chemistry*, 53(6), pp. 1841-1856.

Huang, H., Wang, H., Yih, K., Chang, L. and Chang, T., 2012. Dual Bioactivities of essential oil extracted from the leaves of *Artemisia argyi* as an antimelanogenic versus antioxidant agent and chemical composition analysis by GC/MS. *International Journal of Molecular Sciences*, Vol. 13, pp. 14679-14697.

Huang, L.Q. and Qiu, L., 2014. Abstract: Revision to origin of northern *Artemisia argyi* in Compendium of Materia Medica (Bencao gangmu). *Zhongguo Zhong Yao Za Zhi*. [online] Available at: <https://www.ncbi.nlm.nih.gov/pubmed/25898599> [Accessed 25 March 2017].

Hulla, J.E., Sahu, S.C. and Hayes, A.W., 2015. Nanotechnology: History and future. *Human and Experimental Toxicology*, 34(12), pp. 1318-1321.

Hussain, J.I., Kumar, S., Hashmi, A.A. and Khan, Z., 2011. Silver nanoparticles: preparation, characterization, and kinetics. *Advanced Materials Letters*, 2(3), pp. 188-194.

Hussain, M.A., Shah, A., Jantan, I., Tahir, M.N., Shah, M.R., Ahmed, R. and Bukhari, S.N.A., 2014. One pot light assisted green synthesis, storage and antimicrobial activity of dextran stabilized silver nanoparticles. *Journal of Nanobiotechnology*, 12(53), pp. 1-6.

Ibrahim, H.M.M., 2015. Green synthesis and characterization of silver nanoparticles using banana peel extract and their antimicrobial activity against representative microorganisms. *Journal of Radiation Research and Applied Science*, 8(3), pp. 265-275.

Iravani, S., Korbekandi, H., Mirmohammadi, S.V. and Zolfaghari, B., 2014. Synthesis of silver nanoparticles: chemical, physical and biological methods. *Research in Pharmaceutical Sciences*, 9(6), pp. 385-406.

Irshad, M.D., Zafaryab, M.D., Man Singh and Moshahid Rizvi, M.A., 2012. Comparative analysis of the antioxidant activity of Cassia fistula extracts. *International Journal of Medicinal Chemistry*. [online] Available through:< https://www.hindawi.com/journals/ijmc/2012/157125/> [Accessed on 2 January 2017]

Jain, N., Bhargava, A., Rathi, M., Dilip, R.V. and Panwar, J., 2015. Removal of protein capping enhances the antibacterial efficiency of biosynthesized silver nanoparticles. *PLoS One*. [online] Available at: <https://www.ncbi.nlm.nih.gov/pmc/articles/PMC4520467/> [Accessed 29 March 2017].

James, D.A., Cecilia, G. and Garima, G., 2012. Mugwort (*Artemisia vulgaris*, *Artemisia douglasiana*, *Artemisia argyi*) in the treatment of menopause, premenstrual syndrome, dysmenorrhea and attention deficit hyperactivity disorder. *Scientific research*, Vol. 3, pp. 116-123.

Jang, H., Lim, S.H., Choi, J.S. and Park, Y., 2015. Antibacterial properties of cetyltrimethylammonium bromide-stabilized green silver nanoparticles against methicillin-resistant *Staphylococcus aureus*. *Archives of Pharmacal Research*, 38(10), pp. 1906-1912.

Jindal, H.M.K. and Mohamad, J., 2012. Antioxidant Activity of Ardisia crispa (Mata pelanduk). *Sains Malaysiana*, 41(5), pp. 539-545.

Johnson, A. and Obot, I.B., 2014. Green synthesis of silver nanoparticles using *Artemisia annua* and *Sida acuta* leaves extract and their antimicrobial, antioxidant and corrosion inhibition potentials. *Journal of Materials and Environmental Science*, 5(3), pp. 899-906.

Junglee, S., Urban, L., Sallanon, H. and Lauri, F.L., 2014. Optimized assay for hydrogen peroxide determination in plant tissue using potassium iodide. *American Journal of Analytical Chemistry*, Vol. 5, pp. 730-736.

Jung, W.K., Koo, H.C., Kim, K.W., Shin, S., Kim, S.H. and Park, Y.H., 2008. Antibacterial activity and mechanism of action of the silver ion in *Staphylococcus aureus* and *Escherichia coli. Applied and Environmental Microbiology,* 74(7), pp. 2171-2178.

Jyoti, K., Baunthiyal, M. and Ajeet, S., 2016. Characterization of silver nanoparticles synthesized using *Urtica dioica Linn*. leaves and their synergistic effects with antibiotics. *Journal of Radiation Research and Applied Sciences*, 9(3), pp. 217-227.

Kalainila, P., Subha, V., Ravindran, E.R.S. and Renganathan, S., 2014. Synthesis and characterization of silver nanoparticles from *Erthrina indica. Asian Journal of Pharmaceutical and Clinical Research*, 7(2), pp. 39-43.

Kasote, D.M., Katyare, S.S., Hegde, M.V. and Bae, H.H., 2015. Significance of antioxidant potential in plants and its relevance to therapeutic applications. *International Journal of Biological Sciences*, 11(8), pp. 982-991.

Kawai, M., Hirano, T., Higa, S., Arimitsul, J., Maruta, M., Kuwahara, Y., Ohkawara, T., Higihara, K., Yamadori, T., Shima, Y., Ogate, A., Kawase, I. and Tanaka, T., 2007. Flavonoids and related compounds as anti-allergic substances. Allergology International, 56(2), pp. 113-123.

Kelly, J.M., Keegan, G. and Brennan-Fournet, M.E., 2012. Triangular silver nanoparticles: their preparation functionalisation and properties. *Acta Physica Colona* A, 122 (2), pp, 337–348.

Khalilzadeh, M.A., Borzoo, M., 2016. Green synthesis of silver nanoparticles using onion extract and their application for the preparation of a modified electrode for determination of ascorbic acid. *Journal of Food and Drug Analysis,* 24(4), pp. 796 - 803.

Kheybari, S., Samadi, N., Hosseini, S.V., and Fazeli, A. and Fazeli, M.R.,2010. Synthesis and antimicrobial effects of silver nanoparticles produced by chemical reduction method. *DARU Journal of Pharmaceutical Sciences,* 18(3), pp. 168-172.

Kholoud, M.M., EI-Nour, A., Eftaiha, A., Al-Warthan, A. and Ammar, R.A.A., 2010. Synthesis and applications of silver nanoparticles. *Arabian Journal of Chemistry*, 3(3), pp. 135-140.

Kim, J., Rheem, Y., Yoo, B., Chong, Y., Bozhilov, K.N., Kim, D., Sadowsky, M.J., Hur, H.G., Myung, N.V., 2010. Peptide-mediated shape- and size-tunable synthesis of gold nanostructures. *Acta Biomaterialia*, 6(7), pp. 2681–2689.

Kim, J. Y., Sungeun, K., Kim J., Jongchan L. and Yoon, J., 2005. The biocidal activity of nano-sized silver particles comparing with silver ion. *Journal of Korean Society of Environmental Engineers*, 27(7), pp. 771–776.

Kou, J. and Varma, R.S., 2013. Speedy fabrication of diameter-controlled Ag nanowires using glycerol under microwave irradiation conditions. *Chemical Communication*, 49 (7), pp. 692–694.

Krithika, S., Niraimathi, K.L., Arun, K.P., Narendran, R., Balaji, K. and Brindha, P., 2016. In Vitro Anti-inflammatory studies on silver nanoparticles synthesized from *Centratherum Punctatum Cass. International Journal of Research in Ayurveda and Pharmacy*, 7(2), pp. 61-66.

Kumar, T.M., Christy, A.M.V., Ramya, R.C.S., Malaisamy, M., Sivaraj, C., Arjun, P., Raaman, N. and Balasubramanian, K., 2012. Antioxidant and anticancer activity of *Helicteres isora* dried fruit solvent extracts. *Journal of Academia and Industrial Research*, 1(3), pp. 148 -152.

Lee, K.C., Lin, S.J., Lin, C.H., Tsai, C.S. and Lu, Y.J., 2008. Size effect of Ag nanoparticles on surface plasmon resonance. *Surface and Coatings Technology*, 202(22-23), pp. 5339-5342.

Li, J., Lin, Y.Q. and Zhao, B.G., 2002. Spontaneous agglomeration of silver nanoparticles deposited on carbon film surface. *Journal of Nanoparticle Research*, 4(4), pp. 345-349.

Lim, S.H., Ahn, E.Y. and Park, Y., 2016. Green synthesis and catalytic activity of gold nanoparticles synthesized by *Artemisia capillaris* water extract. *Nanoscale Research Letters*, 11(1), pp. 474.

Liu, Y., Kathan, K., Saad, W. and Prud'hormme, R.K., 2007. Ostwald ripening of ß-carotene nanoparticles. *Physical Review Letters*. [online] Available at: <http://dx.doi.org/10.1103/PhysRevLett.98.036102> [Accessed 2 April 2017].

Lobo, V., Patil, A., Phatak, A. and Chandra, N., 2010. Free radicals, antioxidants and functional foods: Impact on human health. *Pharmacognosy Review*, 4(8), pp. 118-126.

Logeswari, P., Silambarasan, S., Abraham,J., 2012. Synthesis of silver nanoparticles using plants extract and analysis of their antimicrobial property. *Journal of Saudi Chemical Society*, 19(3), pp. 311-317.

Machmudah, S., Wahyudiono, Takada, N., Kanda, H., Sasaki, K. and Goto, M.,2013. Fabrication of gold and silver nanoparticles with pulsed laser ablation under pressurized CO2. *Advances in Natural Sciences: Nanoscience and Nanotechnology*, Vol. 4, pp.1-7.

Mahendran, G.,Kumari R. B.D., 2016. Biological activities of silver nanoparticles from *Nothapodytes nimmoniana (Graham) Mabb.* fruit extracts. *Food Science and Human Wellness*, 5(4), pp. 207-218.

Mahmudin, L., Suharyadi, E., Utomo, A.B.S. and Abraha, K., 2015. Optical properties of silver nanoparticles for surface plasmon resonance (SRP)- based biosensor applications. *Journal of Modern Physics*, Vol. 6, pp .1071-1076.

Maiti, S., Krishnan, D., Barman, G., Ghosh, S.K. and Laha, J.K., 2014. Antimicrobial activities of silver nanoparticles synthesized from *Lycopersicon esculentum* extract. *Journal of Analytical Science and Technology.* [online] Available at: <https://link.springer.com/article/10.1186%2Fs40543-014-0040-3> [Accessed 3 March 2017].

Makarov, V.V., Love, A.J., Sinitsyna,O.V., Makarova,S.S., Yaminsky, I.V., Taliansky, M.E. and Kalinina, N.O., 2014. "Green" Nanotechnologies: Synthesis of metal nanoparticles using plants. *Acta Naturae*, 6(1), pp. 35-44.

Malarkodi, C., Rajeshkumar, S., Paulkumar, K., Gnanajobitha, G., Vanaja, M. and Annadurai, G., 2013. Biosynthesis of semiconductor nanoparticles by using sulfur reducing bacteria *Serratia nematodiphila. Advances in Nano Research*, 1(2), pp. 83–91.

Mansouri, S.S. and Ghader, S., 2009. Experimental study on effect of different parameters on size and shape of triangular silver nanoparticles prepared by a simple and rapid method in aqueous solution. *Arabian Journal of Chemistry*, 2(1), pp. 47-53.

Mlcek, J., Jurikova, Skrovankova, S. and Sochor, J., 2016. Quercetin and its anti-allergic immune response. *Molecules.* [online] Available at: <http://www.mdpi.com/1420-3049/21/5/623> [Accessed 3 February 2017].

Mohan, S.C., Balamurugan, V., Salini, S.T. and Rekha, R., 2012. Metal ion chelating activity and hydrogen peroxide scavenging activity of medicinal plant *Kalanchoe pinnata. Journal of Chemical and Pharmaceutical Research*, 4(1), pp. 197-202.

Molyneux, P., 2004. The use of the stable free radical diphenylpicrylhydrazyl (DPPH) for estimating antioxidant activity. *Journal of Science and Technology*, 26(2), pp. 211-219.

Natalello, A., Ami, D. and Doglia, S.M., 2012. Fourier transform infrared spectroscopy of intrinsically disordered proteins: measurement procedures and data analyses. *Methods in Molecular Biology*, Vol. 895, pp. 229-244.

National Nanotechnology Initiative (NNI). 2000. *"What is Nanotechnology?"*. [online] Available at: <http://www.nano.gov/nanotech-101/what/definition> [Accessed 2 January, 2017].

Neill, S.J., Desikan, R., Clarke, A., Hurst, R. and Hancock, J., 2002. Hydrogen peroxide and nitric oxide as signalling molecules in plants. *Journal of Experimental Botany*, Vol. 53, pp. 1237–1247.

Ogunmoyole, T., Kade, I.J., Johnson, O.D. and Makun, O.J., 2012. Effect of boiling on the phytochemical constituents and antioxidant properties of African pear *Dacryodes edulis* seeds in vitro. *African Journal of Biochemistry Research*, 6(8), pp. 105-114.

Oliveiria, R.N., Mancini, M.C., Oliveira, F.C.S., Passos, T.M., Quilty, B., Thiré, R.M.S. and McGuinness, G.B., 2016. FTIR analysis and quantification of phenols and flavonoids of five commercially available plant extracts used in would healing. *Revista Matéria*, 21(3), pp. 767-779.

Omrani, A.A. and Taghavinia, N., 2011. Photo-induced growth of silver nanoparticles using UV sensitivity of cellulose fibers. *Applied Surface Science*, Vol. 258, pp. 2373-2377.

Patil, S., Rajiv, P. and Sivaraj, R., 2015. An investigation of antioxidant and cytotoxic properties of green synthesized silver nanoparticles. *Indo American journal of pharmaceutical sciences*, 2(10), pp. 1453-1459.

Patra, J.K. and Baek, K.H., 2016. Green synthesis of silver chloride nanoparticles using *Prunus persica* L. outer peel extract and investigation of antibacterial, anticandidal, antioxidant potential. *Green Chemistry Letters and Reviews*, 9(2), pp. 132-142.

Pandey, K.B. and Rizvi, S.I., 2009. Plant polyphenols as dietary antioxidants in human health and disease. *Oxidative Medicine and Cellular Longevity*, 5 (2), pp. 271-278.

Payne, A.C., Mazzer, A., Clarkson, G.J.J. and Taylor, G., 2013. Antioxidant assays-consistent findings from FRAP and ORAC reveal a negative impact of organic cultivation on antioxidant potential in spinach but not watercress or rocket leaves. *Food Science & Nutrition*, 1(6), pp. 439-444.

Pham-Huy, L.A., He, H. and Pham-Huy, C., 2008. Free Radicals, Antioxidants in Disease and Health. *International Journal of Biomedical Science*, 4(2), pp. 89-96.

Phull, A.R., Abbas, Q., Ali, A., Raza, H., Kim, S.J., Zia, M. and Haq, I., 2016. Antioxidant, cytotoxic and antimicrobial activities of green synthesized silver nanoparticles from crude extract of *Bergenia ciliata*. *Future Journal of Pharmaceutical Sciences*, 2(1), pp. 31-36.

Pourjavadi, A. and Soleyman, R., 2011. Novel silver nano-wedges for killing microorganisms. *Materials Research Bulletin*, 46(11), pp. 1860-1865.

Poinern, G.E.J., Chapman, P., Shah, M. and Fawcett, D., 2013. Green biosynthesis of silver nanocubes using the leaf extracts from *Eucalyptus macrocarpa. Nano Bulletin.*, 2 (1), pp. 1–7.

Prabhu, S. and Poulose, E.K., 2012. Silver nanoparticles: mechanism of antimicrobial action, synthesis, medical applications, and toxicity effects. *International Nano Letters*, 2(32), pp. 1-10. [online] Available at: <https://link.springer.com/article/10.1186/2228-5326-2-32> [Accessed 20 March 2017].

Prashith, K.T.R., Akshatha, S., Chaithra, K.J., Priyanka, A., Priyanka, L. and Raghavendra, H.L., 2015. Antimicrobial and radical scavenging activity of leaf and fruit of *Helicteres Isora L. World Journal of Pharmacy and Pharmaceutical Sciences*, 4(7), pp. 1793-1803.

Pyatenko, A., Yamaguchi, M. and Suzuki, M. 2007. Synthesis of spherical silver nanoparticles with controllable sizes in aqueous solutions. *The Journal of Physical Chemistry*, Vol. 111, pp. 7910–7917.

Rahman, S., 2016. Size and concentration analysis of gold nanoparticles with ultraviolet-visible spectroscopy. *Undergraduate Journal of Mathematical Modeling*: One Two, 7(1), pp. 1-13.

Ramachandran, R., Krishnaraj, C., Sivakumar, A.S., Prasannakumar, P., Kumar, V.K.A., Shim, K.S., Song, C.G. and Yun, S.l., 2017. Anticancer activity of biologically synthesized silver and gold nanoparticles on mouse myoblast cancer cells and their toxicity against embryonic zebrafish. *Materials Science and Engineering: C*, Vol. 73, pp. 674 - 683.

Ravishankar, D., Rajora, A.K., Greco, F., Osborn, H.M.I., 2013. Review: Flavonoids as prospective compounds for anti-cancer therapy. *The International Journal of Biochemistry & Cell Biology*, 45(12), pp. 2821-2831.

Rawashdeh, R. and Haik, Y., 2009. Antibacterial mechanism of metallic nanoparticles: A review. *Dynamic Biochemistry, Process Biotechnology and Molecular Biology*, 3(2), pp. 12-20.

Rodriguez-Gattorno, G., Diaz, D., Rendon, L. and Hernandez-Segura, G.O., 2002. Metallic nanoparticles from spontaneous reduction of silver (I) in DMSO. Interaction between nitric oxide and silver nanoparticles. *Journal of Physical Chemistry B*, 106(10), pp. 2482-2487.

Shrivastava1, S., Bera, T., Arnab Roy1, A., Gajendra S., Ramachandrarao, P. and Dash. D., 2007. Characterization of enhanced antibacterial effects of novel silver nanoparticles. *Nanotechnology*, 18(22), pp. 1-9.

Sadeghi, Z., Valizadeh, J., Shermeh, O.A. and Akaberi, M., 2014.Antioxidant activity and total phenolic content of *Boerhavia elegans* (choisy) grown in Baluchestan, Iran. *Avicenna Journal of Phytomedicine*, 5(1), pp. 1-9.

Sakthivel, P. and Anitha, P., 2016. Synthesis and characterization of silver nanoparticles using *Acalypha Indica* leaf extract and its anti-inflammatory activity against human blood cells. *International Journal of Research in Pharmaceutical and Nano Sciences*, 5(1), pp. 26-34.

Salehi, S., Shandiz, S.A.S., Ghanbar, F., Darvish, M.R., Ardestani, M.S., Mirzaie, A. and Jafari, M., 2016. Phytosynthesis of silver nanoparticles using *Artemisia marschalliana* Sprengel aerial part extract and assessment of their antioxidant, anticancer, and antibacterial properties. *International Journal of Nanomedicine*, Vol. 11, pp .1835-1846.

Scholes, G.D., 2010. Quantum-coherent electronic energy transfer: Did Nature think of it first?. *Journal of Physical Chemistry Letters*, 1(1), pp. 2–8.

Settharaksa, S., Madaka, F., Sueree, L., Kittiwisut, S., Sakunpak, A., Moton, C. and Charoenchai, L., 2014. Effect of solvent types on phenolic, flavonoid contennts and antioxidant activities of *Syzygium Gratum* (Wight) S.N.. *International Journal of Pharmacy and Pharmaceutical Sciences,* Vol. 6 (2), pp. 114-116.

Shalaby, E.A. and Shabab, S.M.M., 2012. Comparison of DPPH and ABTS assays for determining antioxidant potential of water and methanol extracts and *Spirulina platensis. Indian Journal of Geo-Marine Sciences*, 42(5), pp. 556-564.

Sharma, K., Ko, E.Y., Assefa, A.D., Ha, S., Nile, S.H., Lee, E.T. and Park, S.W., 2015. Temperature-dependent studies on the total phenolics, flavonoids, antioxidant activities, and sugar content in six onion varieties. *Journal of Food and Drug Analysis*, 23(2), pp. 243-252.

Smitha, S.L., Nissamudeen, K.M., Philip, D. and Gopchandran, K.G., 2008. Studies on surface plasmon resonance and photoluminescence of silver nanoparticles. *Spectrochimica Acta Part A: Molecular and Biomolecular Spectroscopy*, 71(1), pp. 186-190.

Spencer, J.P., Abd El Mohsen, M.M., Minihane, A.M. and Mathers, J.C., 2008. Biomarkers of the intake of dietary polyphenols: strengths, limitations and application in nutrition research. *British Journal of Nutrition*, Vol. 99, pp. 12-22.

Patil, S.P. and Kumbhar, S.T., 2017. Antioxidant, antibacterial and cytotoxic potential of silver nanoparticles synthesized using terpenes rich extract of *Lantana camara* L. leaves. *Biochemistry and Biophysics reports*, Vol. 10, pp. 76-81.

Tajdidzadeh, M., Azmi, B.Z., Mahmood Yunus, W.M., Abizin Talib, Z., Sadrolhosseini, A.R., Karimzadeh, K., Gene, S.A. and Dorraj, M., 2014. Synthesis of silver nanoparticles dispersed in various aqueous media using laser ablation. *The Scientific World Journal*. [online] Available at: <https://www.hindawi.com/journals/tswj/2014/324921/cta/> [Accessed 3 March 2017].

Texeira, J., Gaspar, A., Garrido, E.M., Garrido, J. and Borges, F., 2013. Hydroxycinnamic acid antioxidants: an electrochemical view. *Biomed Research International*, [online] Available at: <http://dx.doi.org/10.1155/2013/251754> [Accessed 4 February 2017].

Tran, Q.H., Nyugen, V.Q. and Le, A.T., 2013. Silver nanoparticles: synthesis, properties, toxicology, applications and perspectives. *Advances in Natural Sciences: Nanoscience and Nanotechnology*, Vol. 4, pp. 1-20.

Valko, M., Leibfritz, D., Moncol, J., Cronin, M.T.D., Mazur, M. and Telser, J., 2007. Free radicals and antioxidants in normal physiological functions and human disease. *The International Journal of Biochemistry & Cell Biology*, 39(1), pp. 44-84.

Van Acker, S.A., de Groot, M.J., van den Berg, D.J., Tromp, M.N., Donne-Op den Kelder G., van der Vijgh W.J. and Bast, A., 1996. A quantum chemical explaination of the antioxidant activity flavonoids. *Chemical Research in Toxicology*, 9(8), pp. 1305-1312.

Vankar, P.S. and Shukla, D., 2012. Biosynthesis of silver nanoparticles using lemon leaves extract and its application for antimicrobial finish on fabric. *Applied Nanoscience*, 2(2), pp. 163- 168.

Velusamy, P., Kumar, G.V., Jeyanthi, v., Das, j. and Pachaiappan,R.,2016. Bio-Inspired green nanoparticles: synthesis, mechanism, and antibacterial application. *Korean Society of Toxicology,* 32(2), pp. 92-102.

Venugopal, K., Rather, H.A., Rajagopal, K., Sheriff, K., Illiyas, M., Rather, R.A., Manikandan, E., Uvarajan, S., Bhaskar, M. and Maaza, M., 2016. Synthesis of silver nanoparticles (Ag NPs) for anticancer activities (MCF 7 breast and A549 lung cell lines) of the crude extract of *Syzygium aromaticum. Journal of Photochemistry and Photobiology B: Biology*, Vol. 167, pp. 282-289.

Verma, A. and Mehata, M.S., 2015. Controllable synthesis of silver nanoparticles using *Neem* leaves and their antimicrobial activity. *Journal of Radiation Research and Applied Sciences*, 9(1), pp. 109-115.

Vetter, T., Iggland, M., Ochsenbein, D.R., Hänseler, F.S., and Mazzotti, M., 2013. Modeling nucleation, growth, and ostwald ripening in crystallization processes: A comparison between population balance and kinetic rate equation. *Crystal Growth & Design*, 13(11), pp. 4890-4905.

Vijayakumar, M., Priya, K., Nancy, F.T., Noorlidah, A. and Ahmed, A.B.A., 2012. Biosynthesis, characterisation and anti-bacterial effect of plant-mediated silver nanoparticles using *Artemisia nilagirica*. *Industrial Crops and Products*, Vol. 41, pp. 235-240.

Wan, C.P., Yu, Y.Y., Zhou, S.R., Liu, W., Tian, S.G. and Cao, S.W., 2011. Antioxidant activity and free radical-scavenging capacity of *Gynura divaricata* leaf extracts at different temperatures. *Pharmacognosy Magazine*, 7(25), pp. 40-45.

Wang, H.S., Qiao, X.Q., Chen, J.G. and Ding, S.Y., 2005. Preparation of silver nanoparticles by chemical reduction method. *Colloids and Surfaces A: Physicochemical and Engineering Aspects*, 256(2-3), pp. 111-115.

Wang, Y.L. and Xia, Y.N., 2004. Bottom-up and top-down approaches to the synthesis of monodispersed spherical colloids of low-melting-points metals. *Nano Letters*, 4(10), pp. 2047-2050.

Wiley, B.J., Chen, Y., McLellan, J.M., Xiong, Y., Li, Z.Y., Ginger,D. and Xia, Y., 2007. Synthesis and optical properties of silver nanobars and nanorice. *Nano Letters*, 7 (4), pp. 1032–1036.

Wong, F.C., Yong, A.L., Ting, E.P.S., Khoo, S.C., Ong, H.C. and Chai, T.T., 2014. Antioxidant, metal chelating, anti-glucosidase activities and phytochemical analysis of selected tropical medicinal plants. *Iranian Journal of Pharmaceutical Research*, 13(4), pp. 1409-1415.

Wright, J.S., Johnson, E.R. and Di Labio, G.A., 2001. Predicting the activity of phenolic antioxidants: theoretical method, analysis of substituent effectss and applications to major families of antioxidants. *Journal of Americal Chemical Society*, 123(6), pp. 1173-1183.

Wu, N. and Sun, Z.D., 2008. Study on antioxidant activity in vitro and protection against DNA oxidative damage of flavonoids of *Artemisia argyi*. *Food Science*, 29 (10), pp. 47–50.

Xie, J. and Schaich, K.M., 2014. Re-evaluation of the 2,2-Diphenyl-1-picrylhydrazyl free radical (DPPH) assay for antioxidant activity. *Journal of Agricultural and Food Chemistry*, 62(19), pp. 4251-4260.

Young, I.S. and Woodside, J.V., 2001. Antioxidants in health and diseas. *Journal of Clinical Pathology,* 54(3), pp. 176-186.

Zhang, H.Y., 2013. Application of silver nanoparticles in drinking water purification. Open Access Dissertations. *Paper 29.* [online] Available at: <http://digitalcommon.uri.edu/oa_diss/29> [Accessed 20 March 2017].

Zhang, P.F., Shi, P.L., Su, J.L., Xue, Y.X., Cao, Z.X., Chu, K.L. and Yan, S.M., 2016. Relieving effect of *Artemisia argyi* aqueous extract on immune

stress in broilers. *Journal of Animal Physiology and Animal Nutrition*, 101(2), pp. 251-258.

Zhang, X.F., Liu, Z.G., Shen, W. and Curunathan, S., 2016. Silver nanopartices: synthesis, characterization, properties, applications, and therapeutic approaches. *International Journal of Molecular Sciences*, 17(9), pp. 1534.

Zhao, F., Shi, B.L., Sun, D.S., Chen, H.Y., Tong, M.M., Zhang, P.F., Guo, X.Y. and Yan, S.M., 2016. Effects of dietary supplmentation of *Artemisia argyi* aqueous extract on antioxidant indexes of small intenstine in broilers. *Animal Nutrition*, 2(3), pp. 198-203.

Zhou, B., Wang, J., Guo, Z., Tan, H. and Zhu, X., 2006. A simple colorimetric method for determination of hydrogen peroxide in plant tissues. *Plant Growth Regulation*, 49(2), pp. 113-118.

Zhu, M.S., Chen P.L., Liu M.H., 2012. Highly efficient visible-light-driven plasmonic photocatalysts based on graphene oxide-hybridized one-dimensional Ag/AgCI heteroarchitectures. *Journal of Materials Chemistry*, 22(40), pp.21487 - 21494.

Zhuravlev, A.V., Zakharov, G.A., Shchegolev, B.F. and Savvateeva-Popova, E.V., 2016. Antioxidant properties of kynurenines: density functional theory calculations. *PLoS Computational Biology.* [online] Available at: <http://journals.plos.org/ploscompbiol/article?id=10.1371/journal.pcbi.1005213> [Accessed 10 February 2017].

APPENDIX A

FTIR analysis of *Artemisia argyi* plant extract